NASA CONTRACTOR REPORT

NASA CR-1884

LOW-CYCLE FATIGUE EVALUATION FOR REGENERATIVELY COOLED PANELS

by C. E. Richard, J. D. Duncan, C. Demogenes, and W. G. Flieder

Prepared by
AIRESEARCH MANUFACTURING COMPANY
Los Angeles, Calif.
for Langley Research Center

NATIONAL AERONAUTICS AND SPACE ADMINISTRATION • WASHINGTON, D. C. • OCTOBER 1971

1. Report No.	2. Government Accession No.	3. Recipient's Catalog No.
NASA CR-1884		

4. Title and Subtitle	5. Report Date
LOW-CYCLE FATIGUE EVALUATION FOR REGENERATIVELY COOLED PANELS	October 1971
	6. Performing Organization Code

7. Author(s)	8. Performing Organization Report No.
C. E. RICHARD, J. D. DUNCAN, C. DEMOGENES, W. G. FLIEDER	68-4313
	10. Work Unit No.

9. Performing Organization Name and Address	11. Contract or Grant No.
AIRESEARCH MANUFACTURING COMPANY A DIVISION OF THE GARRETT CORPORATION LOS ANGELES, CALIFORNIA	NAS 1-5002-4
	13. Type of Report and Period Covered

12. Sponsoring Agency Name and Address	14. Sponsoring Agency Code
NATIONAL AERONAUTICS AND SPACE ADMINISTRATION WASHINGTON, D. C. 20546	

15. Supplementary Notes

16. Abstract

RESULTS OF EXPERIMENTAL LOW-CYCLE FATIGUE EVALUATIONS AT ROOM AND ELEVATED TEMPERATURES OF INCONEL 625 AND HASTELLOY X, BRAZED, PLATE-FIN SANDWICHES SUITABLE FOR REGENERATIVELY COOLED STRUCTURAL PANEL APPLICATIONS ARE PRESENTED AND COMPARED WITH AVAILABLE THEORY. ALSO PRESENTED ARE RESULTS OF SUPPLEMENTAL PARENT METAL TENSILE AND FATIGUE TESTS.

17. Key Words (Suggested by Author(s))	18. Distribution Statement
ELEVATED TEMPERATURE LOW-CYCLE FATIGUE REGENERATIVELY COOLED PANEL FATIGUE BRAZED PLATE-FIN, SUPERALLOY SANDWICH INCONEL 625 HASTELLOY X	UNCLASSIFIED - UNLIMITED

19. Security Classif. (of this report)	20. Security Classif. (of this page)	21. No. of Pages	22. Price*
UNCLASSIFIED	UNCLASSIFIED	72	$ 3.00

*For sale by the National Technical Information Service, Springfield, Virginia 22151

FOREWORD

This report was prepared by AiResearch Manufacturing Company, a division of The Garrett Corporation, Los Angeles, California, for the Langley Research Center of the National Aeronautics and Space Administration. This report presents the results of an experimental study performed under Task Order No. 4, "Low-Cycle Fatigue Evaluation for Regeneratively Cooled Panels". The work is part of a comprehensive analytical and experimental study of regeneratively cooled panels performed under Contract NAS 1-5002. This program was under the cognizance of Mr. R. R. Howell, Dr. M. S. Anderson, Mr. H. N. Kelly and Mr. J. L. Shideler of the High Temperature Structures Branch of the Structures Division, Langley Research Center. The AiResearch program manager was Mr. E. W. Gellersen of the Heat Transfer Project.

LOW-CYCLE FATIGUE EVALUATION

FOR REGENERATIVELY COOLED PANELS

By C.E. Richard, J.D. Duncan, C. Demogenes, and W.G. Flieder
The Garrett Corporation
AiResearch Manufacturing Company

SUMMARY

An experimental low-cycle fatigue evaluation of Hastelloy X and Inconel 625 sheet and sandwich panel specimens was performed to obtain design data for regeneratively cooled panels. A fatigue test apparatus was constructed to apply an alternating strain to a variety of specimen types at room and elevated temperatures. Supplementary tensile test data, including reduction-in-area measurements, provided correlation between predicted and tested fatigue life. Specimens, test conditions, and material selection were based on previous studies of hydrogen-cooled sandwich panels for conditions typical of hypersonic aircraft.

Measurements of reduction in area showed that entrapolation outside of the test range would not be advisable due to ductility variations arising from the material condition. Losses in ductility due to braze alloy coatings were significant particularly at 1540°F (1110°K). Tensile strength changes were less pronounced than those for ductility and the tested strengths were generally comparable to published data.

The parent metal alloys had comparable cycles to failure and room temperature results were in good agreement with current methods of predicting fatigue life. Elevated temperature life was lower than that predicted by theory and the loss was attributed to accumulated creep damage during the load cycle. Furthermore, creep damage apparently dominated at 1540°F (1110°K).

Plate-fin specimens with Hastelloy X brazed with Palniro I and Inconel 625 brazed with Palniro 7 had the highest cycles to failure. As noted for the parent metal specimens, elevated temperature life was reduced by creep damage and sustained strain applications at 1540°F (1110°K) caused additional damage. Overall plate-fin strain concentration factors were estimated to be about 2.4 to 3.0 at room temperature and 1.5 to 1.8 at elevated temperature.

INTRODUCTION

In hypersonic cruise vehicles, regenerative cooling is an attractive thermal protection method for regions with high heating rates for extended operating periods. It was shown in previous analytical studies (reference 1) that sandwich construction provided the desired lightweight construction for such cooled surfaces and a related experimental study (reference 2) verified

that brazed superalloy sandwich panels would be suitable for this application. It was also shown in the reference 1 studies that regeneratively cooled vehicle surfaces would experience strains induced by mechanical loads and restraint of thermal expansion of such magnitude that limited fatigue life could be expected. This experimental low-cycle fatigue study was therefore initiated to compare typical materials and geometries with the objective of providing design data as well as a technique for future fatigue evaluations of sandwich panels.

Previous theoretical estimates of fatigue life (reference 1) were correlated to current theory for metals which relates life to approximately the inverse square of the plastic strain range (cf Manson, reference 3). The proportionality constant between life and strain is generally related to material reduction-in-area or ductility properties (the terms reduction in area and ductility are used interchangeably in this report). However, it was recognized that plate-fin sandwich construction could have significantly different fatigue properties due to braze alloy and geometry effects. Tensile tests of parent metal specimens subjected to braze cycles and coated with braze alloy (reference 2) indicated that the fabricated sandwich materials would have lower ductility and therefore lower fatigue life than the parent material. Also, the plate-fin geometry required for coolant containing passages is known to introduce areas of localized strain concentration. A test apparatus was therefore desired which would permit evaluation and comparison of both parent metal and plate-fin specimens.

The fatigue tests, selected to evaluate the desired configurations, consisted of fully reversed bending of panel (or beam) specimens to controlled strain levels. Although both thermal and mechanical application of strains is expected in actual applications, the mechanical approach was taken to achieve a consistent, repeatable and accurate strain range during sample test life at room and elevated temperatures. One of the primary advantages of mechanical load application is that by testing at a constant temperature we avoid varying material properties due to temperature and simplify the analysis of the results.

Since reduction-in-area properties of the selected alloys were not available in the literature, tensile tests were performed to supply the data required for comparisons between test and theoretical fatigue life. Furthermore, it was assumed that ductility would be sensitive to the effects of the fabrication processes. The tensile tests were therefore performed for a variety of specimens with the appropriate thickness, temperature exposure and braze coating conditions used in the fatigue tests.

Materials, test temperature and plate-fin configuration selection were based on the previous studies (references 1 and 2) of heat exchanger requirements for multiple layer panels. The basic material requirements, besides fabricability, were strength for pressure containment and ductility for low-cycle fatigue capability. Hastelloy X and Inconel 625 provide excellent overall properties as determined from published material property data and fabrication experience. Also, tests of brazed plate-fin sandwiches with Hastelloy X and Inconel 625 verified that the materials provided adequate pressure containment capability.

The temperatures selected for testing were room temperature, 1340°F (1000°K) and 1540°F (1110°K). Based on the reference 1 studies 1540°F (1110°K) appeared to be a reasonable upper limit for superalloy operation in this application. The 1340°F (1000°K) value was selected to investigate the effect of reduced ductility which occurs for most superalloys in the 1200 to 1400°F (920 to 1033°K) temperature range. Room temperature tests were included to aid in machine checkout in the relatively simpler environment and to provide a standard for comparison with the high temperature tests.

SYMBOLS AND PARAMETERS

A constant relating creep life to stress, $(\text{ksi})^{\ell}\text{-sec}$ $\left[(\text{MN/m}^2)^{\ell}\text{-s}\right]$

B constant relating stress to plastic strain, ksi (MN/m^2)

C ductility constant

c power relating cycle life to the plastic strain range

E material elastic modulus, ksi (MN/m^2)

F constant relating creep rate to stress, $(\text{ksi})^{-\ell}\text{-sec}^{-1}$ $\left[(\text{MN/m}^2)^{-\ell}\text{-s}^{-1}\right]$

h specimen height, in. (cm)

h_0 reference specimen height, h_0 = 0.24 in. (0.61 cm)

j number of data points or increments

l power relating creep rate and life to stress

ln logarithm to the base e

log logarithm to the base 10

m strain hardening exponent

N cycles to failure

N' adjusted cycles to failure at the reference specimen height, h_0

R radius, in. (cm)

RA reduction in area, percent

t time, s

t_r time to rupture, s

Δ	increment
ϵ	true strain, percent
ϵ'	engineering strain, percent
$\dot{\epsilon}$	strain rate, percent/s
ϵ_f	fracture ductility, $\epsilon_f = \ell n\ [100/(100-RA)]$
σ	true stress, ksi (MN/m^2)
σ'	engineering stress, ksi (MN/m^2)
Φ	damage

Subscripts

ave	average
C	creep
E	elastic
eq	equivalent
F	fatigue
k	index
m	mandrel
P	plastic
u	ultimate
y	yield
1	specimen length component
2	specimen width component
3	specimen thickness component

TESTS

Tensile tests were performed primarily to obtain material reduction-in-area properties. It was recognized that reduction-in-area measurements can be erratic due to the irregular fracture surface of thin sheet specimens, especially the minimum fatigue specimen metal thickness of 0.010 in. (0.025 cm). For this reason, sheet and wire specimens with a range of thicknesses were tested to determine an acceptable method, or to define the limitations, of measuring the desired reduction-in-area properties. The wire type was included on the assumption that measurements would be more accurate at the smaller thicknesses and that wire data might be extrapolated to cover a range where sheet measurements were unacceptable.

The objective of the fatigue tests was determination of the cycles to failure of a wide variety of parent metal and plate-fin specimens. To satisfy this objective a definition of failure was required which permitted detection of failure when a known, repeatable crack size was produced in the specimen. Furthermore, for comparative life measurements, equal crack sizes at failure are desirable in the various specimen types. Since the predominate fatigue failure mode of plate-fin heat exchangers is evidenced by loss in fluid through a face-sheet crack, loss of internal pressure was the desired means of detection and, consequently, the desired definition of failure in the tests. Crack size, or in this case crack depth, at failure was therefore approximately equal to the face-sheet thickness. Plate-fin specimens and parent metal specimens with a pressurizing cavity utilized this failure criterion by measuring the cycles required to cause loss in gas pressure due to a crack through a 0.010-in. (0.025 cm) section thickness. For solid parent metal specimens (about 0.24-in. (0.61 cm) thickness), failure was defined as complete fracture and it was detected by a significant loss in the load required to bend the specimen. It was observed that when significant load decreases occurred the crack was nearly completely through the specimen and complete fracture into two halves would occur within a few additional cycles. Crack depth was therefore approximately equal to specimen thickness; this is generally referred to as complete fracture or full break of the specimen.

Apparatus

Tensile tests. - The tensile tests were performed on an Instron Universal Testing Machine. The machine has provisions for crosshead movement rates up to 20 in./min. (0.85 cm/s) however, power drive speed capability is an inverse function of load and in some cases the maximum rate was not achievable. Chart speed capability was 50 in/min (2.1 cm/s) and chart and crosshead movements were synchronized for crosshead speeds up to 10 in/min (0.42 cm/s). Peripheral test equipment included a 2.5-in. (6.4 cm) inside diameter Marshall furnace to enclose the specimen for elevated temperature tests and extensometers for direct deflection measurements.

Fatigue tests. - The fatigue tests were performed on an apparatus designed and fabricated for this program. The apparatus, shown in figure 1, applied a known alternating strain by bending the specimen around the opposed curved

mandrel surfaces. A hydraulic ram moved the mandrels through the required stroke while the ends of the specimen were restrained from moving in the direction of ram travel.

The ram was driven by a double acting cylinder of 2.5-in. (6.4 cm) bore utilizing pressures up to 1000 psi (6900 kN/m^2) to provide a total force capability of 4900 lb (21800 N). Ram force levels were monitored by an integral load cell. Stroke reversal was controlled by a four-way solenoid valve and limit switches. Adjustable contacts permitted control of stroke length which was required due to variations in specimen deflection with mandrel radius. Stroke speed was controlled by throttling the flow of hydraulic fluid to the apparatus.

The specimen holding section was designed to fit into an 8-in. (20 cm) inside diameter, Marshall furnace for elevated temperature testing. The resulting sample length was 6 in. (15 cm) and the sample support spacing was 5.1 in. (13 cm). The furnace rests on the support table shown in figure 1a. The heated zone was partially insulated by packing around the base of the furnace which, along with a cooling water jacket around the ram, prevented the load cell from overheating during high temperature tests. The ram head and specimen support section were fabricated from Alloy 713C permitting operation up to about 1700°F (1200°K). The ram is of two-piece construction which permits removal of the head from the top of the apparatus for changing mandrels when necessary. Five pairs of mandrel blocks were fabricated with radii from 2.5 to 32 in. (6 to 81 cm) to give the desired strain range (about 50 to 2000 cycles) for a specimen thickness of 0.24 in. (0.61 cm).

The peripheral equipment included the pump, flow regulator, pressure control system, counter, and control panel. The control system included switches connected in series with the pump which automatically terminated testing either when the specimen cavity pressure decayed below a preset value or when reduced ram hydraulic pressure was sensed.

Specimens

Tensile. - The basic sheet test specimen shown in figure 2 was similar to a standard tensile coupon. Wire specimens were designed with brazed attachment rings; however, they failed at the braze joint and plain wire was used in the tests. Sheet thicknesses and wire diameters varied from 0.008 to 0.114 in. (0.02 to 0.29 cm). Reinforcing tabs were spotwelded to the ends of sheet specimens with thicknesses less than 0.06 in. (0.15 cm) to prevent elongation of the mounting holes. Simulated braze cycles or coating operations were performed prior to machining of the specimens.

Hastelloy X and Inconel 625 were purchased in the mill-annealed condition and metallurgically verified to be within specified composition limits. However re-examination later indicated that one set of coated samples of Inconel X-750 was inadvertently exchanged for Inconel 625. The condition of the material prior to coating application is not known.

Parent metal fatigue. - Two types of parent metal specimens were used during the investigation. The specimen in figure 3a was most representative of the plate-fin specimens since failure detection was also pressure loss through a 0.010-in (0.025 cm) wall thickness (this specimen is referred to as the cavity specimen in subsequent discussions). Cavities were end-milled in two 0.1-in. (0.3 cm) sheets and pressurized to provide two life measurements per specimen. The 0.1-in (0.3 cm) sheets, a 0.04-in (0.10 cm) divider sheet and the pressurizing tubes were brazed with Palniro 7 (70 Au, 8 Pd, 22 Ni) at 1950°F (1340°K) to complete the sample. Specimen height was therefore about 0.24 in. (0.61 cm) and the width was 0.4 in. (1.0 cm) to eliminate biaxial stress effects (see appendix A). Braze alloy was prevented from contacting the 0.010-in. (0.025 cm) test section so that the tensile test properties would be applicable. Finish maching the surface over the cavities was a standard operation; however, additional polishing was also required (see RESULTS AND DISCUSSION section). A 1000 psi (6900 kN/m^2) room temperature pressure test was performed to verify pressure containment capability.

The 2-in. (5 cm) width solid specimen in figure 3b provided a single life measurement based on complete break since load variations due to small surface cracks were not detectable and periodic visual observation, possible at room temperature, was not acceptable at elevated temperatures. The specimens were machined from 0.25-in. (0.64 cm) sheet material and the final grinding operation provided an r.m.s. surface finish of 30 to 60 μ in. (0.8 to 1.5 μ m). Drilled holes of about 0.1-in. (0.3 cm) diameter and 0.12-in. (0.3 cm) depth held the sample in place and provided for thermocouple placement during elevated temperature operations.

Two additional specimens (figures 3c and d) designed to provide information on failure through a 0.010-in. (0.025 cm) section were investigated early in the study. However both gave unsatisfactory results due to wrinkling of the separate sheets (figure 3c) and buckling of the overhanging flange (figure 3d).

Plate-fin fatigue. - The specimen shown in figure 4 had 1.5 by 3.0 in. (4 by 8 cm) cutouts machined on each side of 0.25-in. (0.64 cm) thickness sheet material. Rectangular offset fin sections were inserted in the cutouts and 0.010-in. (0.025 cm) thickness face sheets were placed on each side to complete the sandwich regions and to provide a flat specimen surface. The fin geometry was 20 fins/in. (8 fins/cm) by 0.075-in. (0.19 cm) height by 0.004-in. (0.010 cm) thickness. The facesheet was the minimum considered during the reference 1 studies and the fin design was typical. Independent manifolding of the plate-fin sections provided two measurements of fracture.

Specimens were fabricated from Hastelloy X and Inconel 625, received in the mill-annealed condition, and from Inconel X-750 sheets which were inadvertently substituted for Inconel 625 in one specimen type. Palniro 1 (50 Au, 25 Pd, 25 Ni) and Palniro 7 braze alloys, with brazing temperatures of 2070°F (1410°K) and 1950°F (1340°K), respectively, were used to fabricate the samples. Specimens were held at braze temperature for 1200 s. Cavity pressure capability was verified by a 1500 psi (10300 kN/m^2) room temperature test.

Procedures

Tensile tests. - The load-deflection tests for sheet material were performed in two steps, an initial loading to about 1 percent strain to obtain the yield strength and a second loading to fracture. For the initial loading, an extensometer was attached to the specimen to measure deflection whereas for the second loading, specimen displacement was determined by recording crosshead movement. Loading rates at room temperature were about 0.05 in./min (0.002 cm/s) for the first loading and up to about 5 in./min (0.2 cm/s) for the second. At elevated temperatures, loading rates for the first and second loadings were 0.1 in./min (0.004 cm/s) and 10 in./min (0.4 cm/s), respectively. The elevated temperature test rates were selected to minimize creep relaxation during the cycle. The 0.1 in./min (0.004 cm/s) rate gave the same yield strength value as 0.18 in./min (0.008 cm/s) and permitted accurate termination at about 1 percent total strain. Crosshead rates for the second load cycle of 0.2 to 20 in./min (0.008 to 0.8 cm/s) were investigated with Hastelloy X and the stress-strain curves are shown in figure 5. The ultimate strength increases in each test indicating that creep effects are present at the 10 in./min (0.4 cm/s) rate. However Instron power drive limitations precluded testing all samples at a higher rate.

Wire tests were performed using crosshead movement to measure deflections. Yield strength measurements were not attempted since the smaller wire sizes would not accept an extensometer. Loading rates were the same as for the sheet specimens in the second load cycle.

For elevated temperature measurements the specimens were enclosed in a thermostatically controlled Marshall furnace. Thermocouples located near the specimens indicated that the temperature was controlled to $\pm 10^{\circ}F$ ($6^{\circ}K$).

Fatigue tests. - Specimen load-deflection behavior was established to insure the proper deflection during testing. The central region of the specimen must conform to the mandrel radius to give the known alternating strain. A limited acceptable deflection range existed since insufficient deflection led to reduced strain levels and excessive deflections produced unacceptable strains at the transition from a pressurizing cavity to solid metal or at the edge of a mandrel. A complete load-deflection cycle is illustrated in figure 6a and a typical test curve, utilizing the load cell output and a 0- to 1-in. (2.5 cm) dial indicator to measure ram travel, is shown in figure 6b. Due to the similarity of the materials, particularly their relatively small yield strength variations, a limited number of cycle measurements established performance and maximum load was monitored in subsequent operations. Where required, the load-deflection measurements were taken during the first few cycles using a machine cycle rate of about 0.001 to 0.01 Hz.

The test cycle rate at room temperature was 0.4 to 0.5 Hz. Increases in specimen temperature ($100^{\circ}F$ ($56^{\circ}K$) maximum) during testing indicated that higher rates were undesirable. For the 2-in. (5 cm) width specimens, pump pressure capability was also a limiting factor. The elevated temperature test rate was 0.4 to 0.5 Hz for the cavity parent metal specimens, 0.16 to 0.25 Hz for the

solid specimens, and 0.3 to 0.5 Hz for the plate-fin specimens. In addition, limited elevated temperature plate-fin tests were performed at 0.017 and 0.1 Hz. Based on measurements with thermocouples on the specimens, temperature variations which could be attributed to internal heating were not observed. In hold time tests at 1540°F (1110°K) the above rates were used during the application of load and an automatic timer provided 200 ±10 s holds at maximum specimen deflection (twice per cycle).

For failure detection by loss in pressure, the initial cavity pressure level was 30 to 50 psi (210 to 340 kN/m^2). An automatic shutdown was provided when cavity pressure reduced to 10 to 20 psi (70 to 140 kN/m^2). During room temperature plate-fin tests at the higher strain levels a cavity pressure increase to 300 psi (2100 kN/m^2) was required to prevent fin buckling. The elimination of buckling did not alter the life and therefore tests in which the fins buckled were considered acceptable. In elevated temperature tests, cavity pressure was applied after temperature stabilization to avoid overpressure or creep damage during heating.

Specimen movement across the mandrel was prevented since one end would lose contact with the support roller. Initially the specimen holding section provided the restraint when a pin was placed in the drilled hole (specimens in figures 3b and 4). However specimens were lost when the pin came loose during testing. This difficulty was later avoided by fitting a one-piece clamp over the holding section to restrain the ends of the specimen. Although the hole was therefore not required for restraint, it was still used with the 2-in (5 cm) width specimens to locate a thermocouple in the high temperature zone. The 0.4-in. (1.0 cm) width cavity specimen did not have the drilled hole since the thermocouple was attached to an adjacent spacer bar which positioned this sample on the mandrel.

Initial and final thermocouple readings were recorded for the elevated temperature tests. These measurements indicated that specimen temperature was controlled to within ±10°F (6°K).

RESULTS AND DISCUSSION

Tensile Tests

Tensile properties of Hastelloy X, Inconel 625 and Inconel X-750 were determined for thicknesses, fabrication and processing typical for the fatigue specimens. The primary goal was to obtain reduction-in-area properties so that the fatigue results could be compared to present day theory. The results are summarized in tables 1, 2 and 3 for the three materials. In addition, the Hastelloy X and Inconel 625 sheet yield strengths, ultimate strengths and reduction-in-area properties are shown in figures 7 and 8, respectively, and typical load-deflection curves for as-received material at room temperature, 1340°F (1000°K) and 1540°F (1110°K) are illustrated in figures 9 and 10. The data

reduction method, especially for obtaining reduction-in-area properties, is outlined in appendix A.

Ductility. - The tests showed that due to large ductility variations as a function of material condition extrapolation to untested material states would not be desirable if accurate ductility values were required. This is illustrated in figure 11 by the wide variations in reduction in area obtained for Hastelloy X sheet and wire for a range of thicknesses and diameters. Additional examples of the effects of heat treatment, braze alloy coatings and thickness on Hastelloy X and Inconel 625 ductility can be observed in figures 7a and 8a. Therefore, sheet ductility measurements were used for fatigue life predictions since they provided the closest agreement between the tensile and fatigue test specimen conditions.

As-received sheet: For the 0.11-in. (0.28 cm) sheet material used in the fatigue specimens, Hastelloy X reduction in area was 53 percent at room temperature, decreasing to 43 percent at 1340 and 1540°F (1000 and 1110°K). Inconel 625 reduction in area increased from 43 percent at room temperature to 73 percent at 1540°F (1110°K). Corresponding elongation measurement variations were reported in references 4 and 5 for sheet thicknesses greater than 0.06 in. (0.15 cm). The 0.01-in. (0.03 cm) material had reduced ductility as compared to the 0.11-in. (0.28 cm) sheet, a maximum ductility of 40 percent for Hastelloy X and 49 percent for Inconel 625. Both materials exhibited a small loss in ductility at 1340°F (1000°K) as compared to the other test temperatures for the 0.01 in. (0.03 cm) sheet material.

Simulated braze cycle: The ductility of 0.11-in.(0.28 cm) sheet subjected to the simulated braze cycle at 1925°F (1330°K) differed noticeably from as-received properties. The braze cycle lowered Hastelloy X ductility from 53 to 41 percent at room temperature and from 43 to 38 percent at 1340°F (1000°K) and caused an increase from 43 to 48 percent at 1540°F (1110°K). The largest variation for Inconel 625 was a decrease due to the braze cycle from 73 to 67 percent at 1540°F (1110°K).

Coating tests: The Palniro 1 and Palniro 7 coatings caused significant losses in elevated temperature ductility in the 0.01-in. (0.03 cm) thickness sheet. Palniro 1 had the greater effect, particularly at 1540°F (1110°K) where the ductility reduction from as-received properties was from 40 to 29 percent for Hastelloy X and from 49 to 25 percent for Inconel 625. The maximum losses in ductility due to Palniro 7 were also at 1540°F (1110°K), from 40 to 35 percent for Hastelloy X and from 49 to 40 percent for Inconel 625. Coated Inconel X-750 sheet exhibited a significant loss in ductility at elevated temperatures, about one-half to one-third of Hastelloy X and Inconel 625 values. At room temperature, Inconel X-750 ductility was slightly lower than the other alloys.

Tensile strength. - Yield and ultimate strength variations with sheet thickness and material condition were less pronounced than ductility differences. The general trend was a decrease in tensile properties with decreasing thickness, especially for yield strength. The maximum strength variation with thickness occurred for as-received Inconel 625 at 1340°F (1000°K) when a thickness change from 0.11 to 0.01 in. (0.28 to 0.03 cm) caused a 30 percent yield

strength decrease. Test values compared favorably with published data although the published ultimate strengths were noticeably lower than test values at elevated temperatures. The difference is attributed to the differences in test rate, 0.05 percent/min for reference 5 published data compared to about 400 percent/min in these tests.

The exposure at 1925°F (1330°K) caused up to a 15 percent increase in Hastelloy X ultimate strength and decreases in both yield and ultimate of Inconel 625, up to a maximum of about 30 percent. Palniro 1 and 7 coatings caused relatively minor changes in the Hastelloy X ultimate strength and a maximum increase in yield of 16 percent. Inconel 625 showed minor changes in tensile properties due to the braze alloys. The largest change was a decrease in yield from 43 to 35 ksi (300 to 240 MN/m^2) at 1540°F (1110°K) due to Palniro 1.

Parent Metal Fatigue

The low-cycle fatigue life of Hastelloy X and Inconel 625 parent metal specimens was determined at room temperature, 1340°F (1000°K) and 1540°F (1110°K). The fatigue results for the two specimen configurations are summarized in table 4 for the mandrel radii of 5, 9 and 16 in. (13, 23 and 41 cm) and in figure 12 for the associated plastic strain ranges. The average life values in table 4, used for the data points in figure 12 and subsequent fatigue results curves, are the logarithmic average of the test measurements adjusted to a reference specimen height, h_o. Computations of (true) plastic strain range and the average cycles to failure are discussed in appendix A.

Based on equal applied plastic strain ranges, Hastelloy X and Inconel 625 have comparable cycles to failure, particularly at elevated temperatures (figure 12). A maximum factor of 2 (room temperature data in figure 12a) is considered to be comparable life particularly since the scatter in the data is about the same factor (see below). Comparison of the solid to the cavity specimens should be avoided since significant specimen differences exist such as the machining methods (end mill vs. grinding), the crack depth at failure and other factors discussed below.

Room temperature. - The room temperature fatigue results for the parent metal specimens (polished externally) are compared to current life prediction methods in figures 13 and 14. The measured reduction-in-area properties were used with relations developed by Coffin, Manson, Martin and Morrow which relate cycle life to plastic strain range by

$$N = (C/\varepsilon_p)^c \qquad (1)$$

The power, c, and the relations between the ductility constant, C, and the reduction in area for the applicable references are given in table 5.

The test results are bracketed by the various predictions although they tend to exceed the majority of the predictions especially at the lower values

of the plastic strain range. Absolute values of the slopes of the experimental curves (which ranged from -0.43 and -0.46 for cavity and solid specimens of Inconel 625 respectively to -0.47 for the Hastelloy X specimens) are less than those of the predicted curves which were either -0.5 or -0.6 (predicted slopes are the negative recipocals of the exponent, c, in table 5). Disagreement of the slopes may be due, at least in part, to the effects of cyclic work hardening on the determination of the plastic strain ranges for the experimental data (errors in the determination of the work hardening effects would have a more pronounced effect on the plastic strain ranges at the lower total strain ranges, see appendix A). Cyclic work hardening histories were not obtained during the present investigation. Instead, plastic strain ranges were computed for an assumed work hardening exponent of 0.16 based on experiments with Hastelloy X by Carden and Slade (reference 10) and work with Inconel 713C and Waspaloy by Morrow and Tuler (reference 11).

Best overall agreement between the experimental and predicted life was obtained with the Martin relation (reference 8) although the Manson relation proposed in an addendum to Coffin's paper (reference 6) provides slightly closer agreement with the experimental results for the solid Inconel 625 specimens. The Martin predictions are reproduced in figure 15 together with the experimental data with scatter bands superimposed. It can be seen that the differences between the experimental and predicted data are generally within the scatter band of the experimental data.

The scatter with the cavity specimens displayed a maximum factor (minimum to maximum life) of 2 for Hastelloy X and 1.5 for Inconel 625. The corresponding factors for the solid specimens were 1.1 and 1.3 for Hastelloy X and Inconel 625, respectively. The greater scatter in the cavity type was attributed to lower surface quality. Inconsistent specimen failures were initially experienced with these specimens and subsequent inspection showed that widely spaced scratches were present (the scratches are not defined by standard surface finish measuring techniques, which give an average quality over a section of the surface). External surface polishing prior to testing caused a significant life improvement, however, the scatter was still noticeably greater than had been previously observed with the solid specimens. Therefore, the internal cavity was also polished in a limited number of specimens. Cycle life increases were noted, as well as decrease in the scatter (table 4); however, the improvement did not appear to warrant internal cavity polishing in all specimens. Consequently, externally polished specimens were accepted as standard and data for these specimens are utilized in figures 12, 13 and 15.

Photographs of typical specimens of each type after failure are shown in figure 16. Visual observations of the solid specimens (figure 16b) indicated that the drilled holes for holding the sample and thermocouple caused crack initiation at the edge of the specimen. Specimen life was not significantly reduced by the effects of the hole since independent cracks were observed to occur simultaneously in the central region. Also, it was observed that independent cracks were present adjacent to the main crack (figure 16b) and that first cracks appeared at 70 to 90 percent of the cycles required for full break. Therefore, specimen life could not have been increased by more than 10 to 30 percent if failure had been initiated solely by cracking in the central region.

In addition, the reasonable comparison to predictions in figure 15 suggests that the life reduction was not significant.

Elevated temperatures. - The cycle life curves in figure 12 show large reductions at elevated temperature as compared to room temperature, average life reductions of about 60 percent at 4 percent strain range and 90 percent at 1 percent strain. Relative fatigue life predictions based on reduction-in-area properties do not provide a correlation with these results since, for example, Martin's relation predicts at most a 26 percent life reduction for Hastelloy X and increases in Inconel 625 life. The loss in life was therefore attributed to cumulative creep damage, an effect noted by several investigators including Spera in his recent work on combined creep and fatigue damage (references 12 and 13). Calculations of the creep and fatigue damage fractions, discussed in appendix B, are in reasonable agreement with the test results and the predicted creep damage for Hastelloy X at 1540°F (1110°K) was 75 percent of the total damage at 4 percent plastic strain and 95 percent of the total at 1 percent strain. The life calculations agree with the trends in the elevated temperature test data in that (1) creep damage exceeded fatigue damage for strains greater than 4 percent (2) the creep damage fraction increased at the lower strains (increased creep damage due to longer test life which was not compensated for by the lower stress level) and (3) the straight line relation between log strain and log life exhibited in the tests was duplicated by the calculations.

The elevated temperature cycle life of both alloys was higher in the as-received condition than when they were subjected to the 1925°F (1330°K) cycle. This was attributed to a decrease in creep strength due to the 1925°F (1330°K) cycle since creep was the predominate damage mechanism and no appreciable differences existed between the measured ductilities for the two material conditions.

Plate-Fin Fatigue

Hastelloy X and Inconel 625 plate-fin specimens brazed with Palniro 1 and Palniro 7 were tested at room and elevated temperatures utilizing a fin orientation as shown in figure 4. Specimens with fins 90 degrees to the above orientation were tested using Inconel X-750 facesheets and Inconel 625 fins. The test results are summarized in table 6 and the average fatigue life values were established by the same procedures as for the parent metal samples (see appendix A). The Hastelloy X and Inconel 625 results are also summarized in figure 17. Typical specimen failures are shown in figure 18.

Fatigue life of Hastelloy X specimens brazed with Palniro 1 exceeded those with Palniro 7 by about 50 percent at room temperature although tensile tests indicated that reduction in area of specimens coated with the two alloys were approximately equal. Thus, although reasonable correlation of room temperature parent metal fatigue life to current theory was obtained using measured ductility, the plate-fin results cannot be correlated in this manner. Elevated temperature cycle life was much lower than room temperature life. This is attributed to creep damage rather than reduction-in-area variations as noted for the parent metal tests and discussed in appendix B. Specimens brazed with

Palniro 1 and Palniro 7 had approximately equal cycles to failure at 1540°F (1110°K) and the temperature increase from 1340 to 1540°F (1000 to 1110°K) caused a noticeable life decrease for specimens with Palniro 1. The Hastelloy X-Palniro 1 samples were subjected to a 200 s hold at maximum strain (twice each cycle) in 1540°F (1110°K) tests and the results are also shown in figure 17a. The additional hold caused a decrease in life of up to 60 percent compared to tests without hold time. The loss in life was clearly due to creep damage since the only test variable was the addition of timed sustained strain applications. This shows that steady-state temperature differences which are repeatedly maintained at elevated temperatures can lead to significant material damage. In most elevated temperature operations the transient thermal strains exceed steady-state strains and therefore determine the cycle life. However hold time damage may be particularly important when additional damage occurs during steady-state thermal strains or when this damage dominates that due to transient strains.

For the room temperature Inconel 625 plate-fin tests, specimens brazed with Palniro 7 had about 40 percent greater cycle life than those with Palniro 1. This trend is consistent with, but does not directly relate to the measured reduction in area since ductilities of 37 and 40 percent for Palniro 1 and Palniro 7, respectively, would give the latter a 21 percent higher life by the Martin relation (reference 8). Palniro 7 was also stronger at 1540°F (1110°K), although the curves converge at the lower strain values. The 50 percent difference at 2.5 percent strain may be due primarily to the different measured reduction in areas, 25 and 40 percent for Palniro 1 and Palniro 7 coated coupons, respectively. The two specimen types apparently have similar creep strengths since as creep damage becomes more important at the lower strains (appendix B) the cycle life capabilities converge. The 1340°F (1000°K) curve does not agree with the room temperature results since creep damage should lead to a divergence of the curves at lower strains. The test point at 0.33 percent plastic strain is strongly affected by the yield strength which is a function of the amount of work hardening experienced by the material. The tensile test yield may not be representative of the local material behavior or the assumed 0.16 hardening exponent may not be applicable. The comparison between the 1340 and 1540°F (1000 and 1110°K) tests is consistent with increasing creep damage at the lower strains and higher temperature. However, at the higher strains, where creep is a less important factor, the lower 1340°F (1000°K) life is consistent with the reduction-in-area measurement of the elevated temperature coated coupons.

The Hastelloy X - Palniro 1 and Inconel 625 - Palniro 7 were the strongest of the four plate-fin combinations tested. The comparison in figure 19 (obtained from figure 17) shows that they were of about equal strength at room and elevated temperatures. Figure 19 also provides an indication of the effects of fabrication on fatigue life by comparing the two plate-fin specimens with the cavity parent metal samples (from figure 12). Overall strain concentration factors (ratio of parent metal to plate-fin strain at constant life) can be determined from these curves. At room temperature (figure 19a) the Hastelloy X plate-fin strain concentration is an average of 2.4 whereas the Inconel 625 strain concentration varies from 2.4 at 20 cycles to 3.7 at 500 cycles, an average factor of about 3 (a variable concentration factor frequently occurs for notched specimens tested in the plastic strain region, with the concentration

factor inversely proportional to strain range). At 1540°F (1110°K) the plate-fin and parent metal curves converge at the lower strains indicating that the plate-fin cycle life behavior where creep damage predominates differs appreciably from fatigue behavior. The Hastelloy X plate-fin concentration factor at 1540°F (1110°K) varies from 2.4 at 20 cycles to 1.2 at 500 cycles. The variation for Inconel 625 is less pronounced; from 1.6 at 20 cycles to about 1.4 at 500 cycles. These concentration factors represent an overall reduction in strength due to a combination of braze alloy, geometry, and fabrication effects. Use of these factors to predict performance of plate-fin sandwiches with other fabrication combinations is therefore not recommended, except to give approximate estimates if testing is not feasible.

The predicted fatigue strengths of as-received Inconel 625 and Inconel X-750 are compared to the room temperature plate-fin results in figure 20 using the Martin relation for the predicted curves since it provided the closest life estimates for the parent metal samples. The Inconel 625 results in figure 20a show that the plate-fin curve has an overall strain concentration factor of 2.6 compared to the estimation for as-received 0.01-in. (0.03 cm) sheet (the validity of the as-received estimate is substantiated by the cavity specimen data included in figure 20a). The predicted cycles to failure for Inconel X-750 in the as-received condition and as a plate-fin sandwich with the standard fin orientation are compared to the plate-fin specimens with the 90 degree fin orientation in figure 20b. The Inconel 625 plate-fin strain concentration factor of 2.6 was applied to as-received Inconel X-750 results to estimate Inconel X-750 plate-fin life for the standard fin orientation. When compared to as-received sheet the tests with the 90 degree fin orientation show an average concentration factor of 2 over the 50 to 2000 cycle range. This estimate is dependent on the Inconel X-750 ductility properties; however, with the maximum of 49.5 percent found in the literature (reference 14), the 90 degree fin has about a 20 percent lower concentration factor than the standard fin. This concentration factor of 2 also agrees approximately with a calculated factor for the 90 degree fin of 1.7 to 3.0 based on reversed loading of a tensile bar with 0.010 in. (0.025 cm) thickness (facesheet) for one-quarter to one-half of its length and a 0.014 in. (0.036 cm) section (facesheet plus fin) for one-half to three-fourths of the length. Fin geometry details leading to concentration factors that are a function of orientation can be seen in figure 4. These comparative results for the two fin orientations indicate that the standard orientation produces the lowest life.

If the strain concentration factor discussed above could be separated into a factor for each fabrication process, reduced testing would be required to obtain design data. However these limited evaluations indicate that braze alloy and geometrical effects are not independent. For example, the Inconel 625 plate-fin data in figure 20a indicates that plate-fin life reductions are primarily attributable to geometrical effects since the predicted and tested cycles to failure of as-received, braze cycle and coated sheet are in close agreement. However, in a similar comparison for Inconel X-750 in figure 20b the geometrical strain concentration factor for the standard fin would be about 1.5 (standard fin vs Palniro 7 coated sheet) compared to 2.6 estimated for combined fabrication effects. Since fatigue tests were not performed on coated parent metal the validity of using the coated sheet ductility measurements to estimate life of

the coated material was not determined. However the test results demonstrate that the correlation would not be adequate for predicting the separate effect of braze alloy application. Also, as noted above, the room temperature plate-fin results did not correlate to relative measured ductility properties of Palniro 1 and Palniro 7 coated tensile coupons. The lack of correlation between coated specimen ductility and fatigue life would be expected if fatigue life were dependent on material behavior in a localized region whereas coated sheet tensile tests produce average ductility properties in the fracture region.

CONCLUDING REMARKS

An experimental low-cycle fatigue evaluation of Hastelloy X and Inconel 625 sheet and sandwich panel specimens has been performed to provide design data for regeneratively cooled panels. A test apparatus was designed and constructed to apply an alternating strain to a variety of parent metal and plate-fin sandwich specimens at room temperature, 1340°F (1000°K) and 1540°F (1110°K). Reduction-in-area properties, obtained from supplementary tensile tests of the desired sheet thicknesses, were used to correlate the fatigue results to current prediction methods. Specimen configuration, test conditions, and material selection were based on previous analytical and experimental studies of regeneratively cooled panels reported in references 1 and 2.

Reduction-in-area measurements of tensile test specimens showed variations due to thickness, fabricating method, heat treatment and a surface coating of such magnitude that extrapolation outside the test range would not be desirable for accurate ductility estimates. Braze alloy coated specimens of 0.01-in. (0.03 cm) thickness showed significant losses in ductility as compared to as-received sheet. The major reductions occurred at the 1540°F (1110°K) test temperature with the Palniro 1 braze alloy.

Tensile strength changes with thickness and material condition were less pronounced than the ductility variations. Test results were comparable to published data, although the tested ultimate strengths at elevated temperatures were higher due to a faster test loading rate. The 1925°F (1330°K) simulated braze cycle caused increased Hastelloy X ultimate strength and decreases in yield of both alloys. Braze alloy coatings generally reduced specimen tensile strength.

Hastelloy X and Inconel 625 parent metals had comparable cycles to failure based on equal applied plastic strain ranges. Room temperature fatigue results compared favorably to current life predictions based on measured material reduction in areas. There was a significant loss in life at elevated temperature relative to room temperature. This reduction cannot be explained on the basis of current fatigue theory and it was attributed to accumulated creep damage during the load cycle. Furthermore, creep damage was apparently the dominating failure mechanism at 1540°F (1110°K).

The plate-fin cycles to failure of Hastelloy X brazed with Palniro 1 and Inconel 625 brazed with Palniro 7 were generally superior to the other material

combinations over the entire temperature range. As noted for the parent metal specimens, elevated temperature life was greatly reduced due to creep damage. Timed holds at maximum strain at 1540°F (1110°K) caused significant life reductions indicating that steady-state thermal strains for repeated extended operating times could govern cycle life design.

The plate-fin specimen combinations exhibited overall strain concentration factors of 2.4 to 3.0 at room temperature and 1.5 to 1.8 at elevated temperature. These concentration factors represented an accumulation of the effects of braze alloy, geometry, and fabrication; the test results indicate that separation of the effects is not presently feasible and that fatigue tests of the fabricated plate-fin sandwich are required for accurate life estimates.

APPENDIX A

DATA REDUCTION

Tensile Tests

Reduction in area. - Specimen thickness or diameter was determined to within 0.0001 in. (0.0003 cm) prior to testing. Subsequent to failure, the thickness of both sides of the fracture was measured with a hand micrometer (anvil tip). The micrometer thickness measurements were taken 0.01 to 0.03 in. (0.03 to 0.08 cm) from the edge of the fracture since the fracture face was not always perpendicular to the plane of the specimen. The area reduction was gradual along the specimen rather than local at the fracture zone so the error in measurement was within the accuracy of the initial thickness measurements. However, as specimen thickness decreased there was increased uncertainity in the computed ductility because decreasing thickness changes were measured with constant precision. Optical measurements were also attempted; however, the accuracy did not exceed that of the micrometer measurements since at the required magnification the limited depth of focus prevented accurate definition of the irregular edge of the specimen.

For the sheet specimens, thickness measurements were taken at five locations across the width on either side of the fracture. The five locations were approximately equispaced. Sample width was obtained by placing the fractured pieces together and measuring the minimum value. A typical set of measurements shown in table 7 indicates the sample variations such as preferential thinning at the center of the specimen due to biaxial stress effects.

Wire diameters were measured at two locations, rotated 90 degress from one another. Otherwise the wire measuring technique was identical to that used for sheet specimens.

Elongation. - Sheet elongation after fracture was obtained by fitting the failed sections together and measuring the distance between extensometer marks. Initial separation of the marks (gauge length) was 2 in. (5 cm) except for the 0.01-and 0.02-in. (0.03 and 0.05 cm) thickness material which had the extensometer marks outside the constant width section to avoid failure at the gauge marks in the elevated temperature tests. This introduced an error in elongation measurements of about 10 percent due to the increased width of the specimen at either end of the longer gauge length.

Wire elongation was also obtained by fitting the sample sections together after failure. Scribe marks, applied prior to testing, provided the reference measuring points.

Yield and ultimate tensile strength. - Yield strength was determined at the 0.2 percent offset plastic strain point as measured on the initial extensometer load-deflection curve used for the sheet specimens. Yield was not

measured for the wire samples since extensometer measurements were not obtained. Ultimate strength was the maximum stress value attained by the tensile coupon.

Fatigue Tests

Plastic strain range. - When the specimen conforms to the mandrel radius, the applied total engineering strain in the specimen length dimension, ε_l', is related to overall specimen height and mandrel radius by

$$\varepsilon_l' = h/(R_m + 0.5h) \tag{2}$$

The general relation between true and engineering strains

$$\varepsilon = \ln (1 + \varepsilon') \tag{3}$$

is used to convert to the total true strain component, ε_l, since the desired true strains are noticeably different from engineering strains at the tested strain levels. Subsequent computations of true plastic strain ranges were determined from the total true strain for the beam and plate specimens utilizing material stress-strain properties for the repeating cycle shown in figure 21. The total strain range shown in figure 21 consists of twice the elastic strain plus the plastic strain so material stress-strain behavior was correlated to the loading curve from points 4 to 1. The compressive stress-strain curve is assumed to be identical to the tensile curve. The resulting (true) plastic strain ranges are summarized for the four specimen types in table 8, and the associated material engineering properties from the tensile tests and published data are presented in table 9. The engineering properties were converted to true stress-strain values by the power law relation which accurately describes uniaxial true stress-strain behavior.

$$\sigma = B\,\varepsilon_P^m \tag{4}$$

A strain hardening exponent, m, of 0.16 accounts for cyclic material behavior. Assuming that ultimate strength is not affected by cyclic hardening or softening, the constant, B, is

$$B = \sigma_u'\, e^m/(m)^m \tag{5}$$

The factor, e^m, converts engineering ultimate to the equivalent true stress at the tensile instability strain, m.

Beam behavior: The 0.4-in. (1.0 cm) width cavity parent metal specimen performed as a beam in bending. This was verified by stresscoat and strain gauge tests performed at room temperature on a 0.6-in. (1.5 cm) width specimen shown in figure 22. The stresscoat pattern shows lateral cracks, indicating uniform stress across the width, and the measured strains agreed with the total

strains calculated from equation 2. For beam behavior, the cycle for the lengthwise components (figure 21) is the same as for uniaxial loading so the plastic strain component, ϵ_{1P}, is the desired plastic strain range ϵ_P. The total uniaxial strain is therefore related to true stress by

$$\epsilon_1 = 2\epsilon_{1E} + \epsilon_P = \frac{2\sigma}{E} + \left(\frac{\sigma}{B}\right)^{1/m} \tag{6}$$

Equations 4 and 6 permit calculation of plastic strain ranges (table 8) from the uniaxial total strain by the equation

$$\epsilon_P + \frac{2B\epsilon_P^m}{E} = \epsilon_1 \tag{7}$$

Plate behavior: The 2-in. (5 cm) width solid parent metal and plate-fin specimens were held flat by the mandrels in the central region. This produces a biaxial stress state with the condition that the total strain in the width, ϵ_2, is equal to zero. This loading was substantiated by discoloration of the sample where mandrel contact occurred (see figure 16 b). The resulting stress and strain components must be converted to the equivalent stress and strain which correspond to uniaxial tensile behavior (equation 4). The equivalent strain range is desired since present failure theory relates the equivalent plastic strain to fatigue life. From deformation theory (Mises criterion) equivalent true stress is related to the true biaxial components by

$$\sigma_{eq} = (\sigma_1^2 - \sigma_1\sigma_2 + \sigma_2^2)^{1/2} \tag{8}$$

The true equivalent plastic strain is a function of true plastic strain components, given by

$$\epsilon_{eq} = (\sqrt{2/3})[(\epsilon_{1P}-\epsilon_{2P})^2 + (\epsilon_{2P}-\epsilon_{3P})^2 + (\epsilon_{3P}-\epsilon_{1P})^2]^{1/2} \tag{9}$$

The relation between total strain in the length, ϵ_1, and plastic strain range was obtained by an incremental calculation of the biaxial stress-strain curve. Values of plastic strain were selected, and equation 4 gives the equivalent stress. The boundary condition

$$\epsilon_2 = \epsilon_{2E} + \epsilon_{2P} = 0 \tag{10}$$

combined with elastic and plastic stress-strain relations determines the approximate ratio between σ_1 and σ_2. The desired (equivalent) plastic strain was obtained at the applied total strain component, ϵ_1, associated with the mandrel radii.

Cycles to failure. - The test cycle life was adjusted to give specimen life for a common reference height, h_o, of 0.24 in. (0.61 cm). This permitted computation of plastic strains at the single specimen height. The adjusted cycle life, N′, was related to test life, N, through equation 2, by the approximation

$$N' = N\,(h/h_o)^2 \tag{11}$$

The logarithmic average of a set of data points, j, is

$$N'_{ave} = 10^{\left(\frac{1}{j}\sum_{o}^{j} \log N'_k\right)} \tag{12}$$

APPENDIX B

CREEP EFFECTS

Recent work by Spera (references 12 and 13) illustrates the importance of creep damage during high temperature cyclic loading and estimates creep and fatigue damage to explain a considerable variety of high temperature cyclic test data. His work shows that the Robinson-Tiara linear creep damage theory gives reasonable correlation to the data. The suggested general expression for combined creep and fatigue damage per cycle is then the summation of cycle and time increments divided by the life for each load level, j.

$$\Delta\Phi = \Delta\Phi_F + \Delta\Phi_C = \sum_{o}^{j} \frac{\Delta N_k}{N_{F,k}} + \sum_{o}^{j} \frac{\Delta t_k}{t_{r,k}} \tag{13}$$

Failure is assumed when

$$\sum \Delta\Phi = 1 \tag{14}$$

The fatigue damage fraction in equation 13 for a constant plastic strain amplitude during the life, using the Martin parameters in equation 1, is

$$\Delta\Phi_F = (\epsilon_p/C)^2 \tag{15}$$

The creep damage fraction was evaluated for Hastelloy X under several test conditions to estimate the combined damage. The resulting cyclic life was then compared to the test data.

Typical thermal or mechanical load cycles at elevated temperatures cause creep damage during strain application and sustained strains. The associated creep relaxation leads to a modified stress-strain curve both during loading and at constant strain. A typical completely reversed stress-strain cycle illustrating both relaxation effects is shown in figure 23a. The stress history for the unrelaxed stress-strain curve was based on equation 4. Stress relaxation and damage were estimated from standard engineering property data for the 1 percent creep and rupture stress. Creep rate and life at the desired temperature were related to stress by the power law expressions.

$$\dot{\epsilon} = F\sigma^{\ell} \tag{16}$$

$$t_r = A\sigma^{-\ell} \tag{17}$$

The creep damage per cycle, from equations 13 and 17, is therefore

$$\Delta\Phi_c = \int_o^t \frac{\sigma^{\ell}\, dt}{A} \qquad (18)$$

where equation 16 determines the stress history. A linear creep rate was assumed to a strain of 1 percent since creep strain vs time curves were not available for Hastelloy X (of the two alloys, Hastelloy X published property data exceeds that of Inconel 625). As discussed below, the use of engineering creep data introduces errors in both creep rate and creep life estimates. The simplified uniaxial tensile loading shown in figure 23b was used to compute damage rather than the more exact cycle in figure 23a, which has an increased plastic strain range due to creep relaxation. Equal tensile and compressive damage were also assumed although Spera (reference 13) recommends ignoring the compressive sustained strain application. The damage estimates for the sustained strains in the parent metal tests are not of sufficient accuracy to evaluate the importance of that assumption.

The calculations were based on parent metal tensile properties listed in tables 9a and b, and creep constants (equations 16 and 17) in table 9c for as-received Hastelloy X (reference 4). The half-cycle loading times were 0.5 and 1.0 s for the cavity and solid specimens, respectively. In addition, sustained strain hold times of 0.05 and 0.1 s were assumed for the respective specimen types. This short duration hold occurs in the center of the specimen during every half-cycle due to the additional time required to reach maximum strain in adjacent sections. These times were based on the load history in figure 6 using cycle rates of 0.5 and 0.25 Hz.

The tested and estimated cycles to failure in the 1340 to 1540°F (1000 to 1110°K) temperature range are shown in figure 24a. The predicted cycles to failure for the two specimen types are about equal whereas the test values show the solid specimen to be stronger. This discrepancy may be attributed to variations in creep strength of the cavity specimens due to the simulated braze cycle since the test values at room temperature do not show the same trend. The calculations were performed for as-received creep properties since the effects of the braze cycle were not evaluated. The estimates indicate a more severe loss in cycle life than the test results as the temperature increases. The predictions also overestimate the life at the lower temperature and underestimate life at 1540°F (1110°K). As discussed below the engineering creep property data is not suitable for computing relaxation or life; however, the effect on the relation between estimates and tests of improved data (or data usage) is not clear in this case.

Tested and predicted cycles to failure vs plastic strain range are shown in figure 24b. The straight line relationship between log strain and log cycles exhibited by the test results is duplicated by the estimating method. The slope of the life estimates exceeds the test slope; however, reasonable agreement exists between cycles to failure for test and theory for the cavity specimens. The calculated creep damage was about 75 percent of the total damage at 4 percent

strain and 95 percent at 1 percent strain. The predicted life of the solid specimens is about two-thirds of the test values at 4 percent strain and about one-fourth at 1 percent plastic strain. The discrepancy between calculated life and test values might be reduced by improving the calculation of stress relaxation during the cycle and by an improved relationship between creep life and stress. Comparison of the calculated relaxation and stress-strain rate effects shown in figure 5 indicated that the amount of relaxation is overestimated. This is partially attributed to the use of the linear creep rate relation obtained from standard engineering creep data which results in an underestimation of the creep rate at lower strains and an overestimate at higher strains. As discussed by Lubahn and Felgar (reference 15) true creep strain rate diminishes steadily with time due to strain hardening in the standard constant load creep test. Since Hastelloy X exhibited strain hardening at elevated temperatures, similar behavior would be expected. Creep strain vs time curves, not available for Hastelloy X or Inconel 625, are required to determine a more accurate relation between creep rate, time, and plastic strain. In addition, the standard stress-rupture test data is obtained from a constant load test so the creep life is evaluated under an increasing stress level. The standard engineering data, based on the initial stress, therefore predicts lower life than would be expected under a constant stress test. Since strain (stress) was controlled during the fatigue tests the constant stress data would be more representative for these estimates. Improvements in the material data would presumably improve the life estimates although current creep theory and combined creep and fatigue understanding are not sufficient for performing accurate life estimates.

Figure 24c illustrates the effects of cycling rate on the life of the material. The limited test data does not show a definite trend over the ranges of cycle times; however, calculated life cycles diminish as cycle time increases. Equation 18 predicts a linear relation between creep damage and cycle time when stress relaxation effects are not considered. When noticeable stress relaxation occurs, as was the case for the calculations at the longer cycle times, the damage due to the increased time duration is partially compensated for by the lower average stress during the cycle.

REFERENCES

1. Flieder, W.G.; Richard, C.E.; Buchmann, O.A.; and Walters, F.M.: An Analytical Study of Hydrogen Cooled Panels for Application to Hypersonic Aircraft. NASA-CR1650, April 1970.

2. Demogenes, C.; Jones, O.; Richard, C.E.; Duncan, J.D.; and Flieder, W.G.: Fabrication and Structural Evaluation for Regeneratively Cooled Panels. NASA-CR1651, March 1970.

3. Manson, S.S.: Fatigue: A Complex Subject -- Some Simple Approximations. Experimental Mechanics, July 1965.

4. Anon: Hastelloy Alloy X. Report F30,037D, Union Carbide Corporation, Stellite Division, October 1964.

5. Anon: Engineering Properties of Inconel Alloy 625. Report T-42, International Nickel Company, August 1966.

6. Tavernelli, J.F. and Coffin, L.F., Jr: Experimental Support for Generalized Equation Predicting Low Cycle Fatigue. Journal of Basic Engineering, December 1962.

7. Manson, S.S.: Thermal Stress and Low-Cycle Fatigue. McGraw-Hill Book Company, 1966.

8. Martin, D.E.: An Energy Criterion for Low-Cycle Fatigue. Journal of Basic Engineering, December 1961.

9. Morrow, JoDean: Cyclic Plastic Strain Energy and Fatigue of Metals. STP 378, American Society of Testing and Materials, 1965.

10. Carden, A.E. and Slade, T.B.: High Temperature Low-Cycle Fatigue Experiments on Hastelloy X. ASTM STP 459, American Society for Testing and Materials, 1969.

11. Morrow, JoDean and Tuler, F.R.: Low Cycle Fatigue Evaluation of Inconel 713C and Waspaloy. Journal of Basic Engineering, June 1965.

12. Spera, D.A.: The Calculation of Elevated-Temperature Cyclic Life Considering Low Cycle Fatigue and Creep. NASA TN D-5317, July 1969.

13. Spera, D.A.: Calculation of Thermal-Fatigue Life Based on Accumulated Creep Damage. NASA TN D-5489, October 1969.

14. Anon: Engineering Properties of Inconel Alloy X-750. Report T-38, International Nickel Company, 1963.

15. Lubahn, J.D. and Felgar, R.P.: Plasticity and Creep of Metals. John Wiley and Sons, 1961.

TABLE I

HASTELLOY X TENSILE TEST RESULTS

a. 1540°F(1110°K) AS-RECEIVED SHEET AT FOUR CROSSHEAD SPEEDS

Crosshead rate, in./min (cm/s)	Initial dimensions, in.(cm)		Ultimate strength, ksi (MN/m^2)	Yield strength, ksi (MN/m^2)	Elongation, percent	Reduction in area, percent
	Width	Thickness				
0.2(0.01)	0.50(1.3)	0.010(0.025)	41(280)	30(210)	47	46
3.0(.13)			56(390)	31(210)	39	42
5.0(.21)			57(390)	30(210)	36	44
20.0(.85)			62(430)	30(210)	35	44

NOTE: (1) Gauge length was 2 in. (5 cm) except that at elevated temperature the gauge length for 0.01- and 0.02-in. (0.03 and 0.05 cm) sheet was about 2.5 in. (6.4 cm).

b. AS-RECEIVED SHEET, 10 IN/MIN (0.42 cm/s) CROSSHEAD SPEED AT ELEVATED TEMPERATURES

Temperature, °F(°K)	Initial dimensions, in.(cm)		Ultimate strength, ksi (MN/m^2)		Yield strength, ksi (MN/m^2)		Elongation, percent		Reduction in area, percent	
	Width	Thickness	Test	Average	Test	Average	Test	Average	Test	Average
Room temperature	0.50(1.3)	0.113(0.287)	109(750)		54(370)		47		52	
	.50(1.3)	.113(.287)	108(740)	109(750)	54(370)	54(370)	45	46	54	53
	.42(1.1)	.113(.287)	109(750)		54(370)		45		52	
	0.50(1.3)	0.063(0.160)	104(720)		49(340)		48		47	
			104(720)	104(720)	49(340)	49(340)	47	48	46	47
			104(720		49(340)		48		48	
	0.50(1.3)	0.042(0.107)	111(770)		51(350)		46		49	
			109(750)	110(760)	49(340)	49(340)	45	45	49	48
			109(750)		48(330)		45		47	
	0.50(1.3)	0.023(0.058)	105(720)		51(350)		50		43	
			106(730)	105(720)	51(350)	51(350)	49	49	45	45
			105(720)		51(350)		48		46	
	0.50(1.3	0.010(0.025)	115(790)		51(350)		37		33	
			116(800)	116(800)	51(350)	50(340)	41	39	35	34
			116(800)		49(340)		40		35	
1340(1000)	0.50(1.3)	0.113(0.287)	73(500)		36(250)		44		44	
			74(510)	73(500)	36(250)	36(250)	44	44	41	43
			73(500)		35(240)		45		43	
	0.50(1.3)	0.063(0.160)	73(500)		34(230)		41		44	
			73(500)	72(500)	34(230)	34(230)	42	42	42	43
			70(480)		33(230)		44		44	
	0.50(1.3)	0.042(0.107)	74(510)		30(210)		42		42	
			75(520)	75(520)	31(210)	31(210)	43	43	42	41
			76(520)		31(210)		43		38	

NOTE: (1) Gauge length was 2 in. (5 cm) except that at elevated temperature the gauge length for 0.01- and 0.02-in. (0.03 and 0.05 cm) sheet was about 2.5 in. (6.4 cm).

TABLE I. Continued

b. AS-RECEIVED SHEET, 10 IN/MIN (0.42 cm/s) CROSSHEAD SPEED AT ELEVATED TEMPERATURES (Continued)

Temperature, °F(°K)	Initial dimensions, in.(cm)		Ultimate strength, ksi (MN/m^2)		Yield strength, ksi (MN/m^2)		Elongation, percent		Reduction in area, percent	
	Width	Thickness	Test	Average	Test	Average	Test	Average	Test	Average
1340(1000)	0.50(1.3)	0.023(0.058)	72(500)		34(230)		44		41	
			73(500)	72(500)	34(230)	33(230)	44	45	39	39
			72(500)		32(220)		47		38	
	0.050(1.3)	0.010(0.025)	78(540)		33(230)		35		32	
			78(540)	78(540)	33(230)	33(230)	36	35	32	32
			78(540)		34(230)		34		32	
1540(1110)	0.43(1.1)	0.113(0.287)	61(420)		35(240)		35		41	
	.43(1.1)		62(430)	62(430)	35(240)	35(240)	38	37	45	43
	.50(1.3)		62(430)		35(240)		37		43	
	0.50(1.3)	0.063(0.160)	61(420)		33(220)		40		57	
			60(410)	60(410)	32(220)	32(220)	45	44	55	56
			60(410)		32(220)		48		56	
	0.43(1.1)	0.042(0.107)	60(410)		32(220)		44		49	
	.50(1.3)		59(410)	60(410)	28(190)	30(210)	46	45	51	50
	.49(1.2)		60(410)		29(200)		45		51	
	0.50(1.3)	0.023(0.058)	61(420)		32(220)		37		48	
			60(410)	60(410)	31(210)	32(220)	38	37	49	49
			61(420)		32(220)		36		49	
	0.50(1.3)	0.010(0.025)	59(410)		30(210)		36		43	
			61(420)	61(420)	30(210)	30(210)	37	36	37	40
			62(430)		31(210)		36		39	

NOTE: (1) Gauge length was 2 in. (5 cm) except that at elevated temperature the gauge length for 0.01- and 0.02-in. (0.03 and 0.05 cm) sheet was about 2.5 in. (6.4 cm).

c. AS-RECEIVED SHEET WITH 1925°F(1330°K) SOAK FOR 300 SECONDS

Temperature, °F(°K)	Initial dimensions, in.(cm)		Ultimate strength, ksi (MN/m^2)		Yield strength, ksi (MN/m^2)		Elongation, percent		Reduction in area, percent	
	Width	Thickness	Test	Average	Test	Average	Test	Average	Test	Average
Room temperature	0.50(1.3)	0.113(0.287)	118(810)		54(370)		35		42	
			118(810)	118(810)	55(380)	55(380)	35	35	41	41
			119(820)		56(390)		35		40	
1340(1000)	0.50(1.3)	0.113(0.287)	85(590)		36(250)		31		38	
			84(580)	84(580)	36(250)	36(250)	31	31	37	38
			82(570)		35(240)		30		39	
1540(1110)	0.50(1.3)	0.113(0.287)	67(460)		34(230)		40		49	
			66(460)		34(230)		42		50	
			66(460)	66(460)	-(2)	34(230)	36	37	47	48
			66(460)		34(230)		24		48	
			66(460)		34(230)		35		45	
			67(460)		34(230)		32		48	

NOTES: (1) Gauge length was 2 in. (5 cm) except that at elevated temperature the gauge length for 0.01- and 0.02-in. (0.03 and 0.05 cm) sheet was about 2.5 in. (6.4 cm).
(2) Extensometer grips moved during test.

TABLE I. Continued

d. COATED WITH PALNIRO I

Temperature, °F(°K)	Initial dimensions, in.(cm)		Ultimate strength, ksi (MN/m^2)		Yield strength, ksi (MN/m^2)		Elongation, percent		Reduction in area, percent	
	Width	Thickness	Test	Average	Test	Average	Test	Average	Test	Average
Room temperature	0.50(1.3)	0.011(0.028)	123(850)		59(410)		24		33	
			120(830)	122(840)	57(390)	58(400)	29	27	33	33
			123(850)		58(400)		29		34	
1340(1000)	0.50(1.3)	0.011(0.028)	82(570)		37(260)		19		21	
			83(570)	80(550)	34(230)	34(230)	27	23	23	24
			74(510)		32(220)		22		27	
1540(1110)	0.50(1.3)	0.011(0.028)	59(410)		30(210)		28		27	
			63(430)	59(410)	31(210)	29(200)	33	28	29	29
			55(380)		28(190)		24		30	

NOTE: (1) Gauge length was 2 in. (5 cm) except that at elevated temperature the gauge length for 0.01-and 0.02-in. (0.03 and 0.05 cm) sheet was about 2.5 in. (6.4 cm).

e. COATED WITH PALNIRO 7

Temperature, °F(°K)	Initial dimensions, in.(cm)		Ultimate strength, ksi (MN/m^2)		Yield strength, ksi (MN/m^2)		Elongation percent		Reduction in area, percent	
	Width	Thickness	Test	Average	Test	Average	Test	Average	Test	Average
Room temperature	0.50(1.3)	0.011(0.028)	123(850)		56(390)		34		35	
			123(850)	123(850)	56(390)	56(390)	34	35	35	35
			123(850)		55(380)		36		36	
1340(1000)	0.50(1.3)	0.011(0.028)	75(520)		31(210)		33		34	
			75(520)	75(520)	30(210)	31(210)	35	31	35	32
			75(520)		31(210)		24		28	
1540(1110)	0.50(1.3)	0.011(0.028)	62(430)		30(210)		33		33	
			61(420)	60(410)	30(210)	29(200)	27	30	34	35
			56(390)		27(190)		31		37	

NOTE: (1) Gauge length was 2 in. (5 cm) except that at elevated temperature the gauge length for 0.01-and 0.02-in. (0.03 and 0.05 cm) sheet was about 2.5 in. (6.4 cm).

f. AS-RECEIVED WIRE, 10 IN./MIN (0.42 cm/s) CROSSHEAD SPEED AT ELEVATED TEMPERATURES

Temperature, °F(°K)	Initial diameter, in.(cm)	Ultimate strength, ksi (MN/m^2)		Elongation, percent		Reduction in area, percent	
		Test	Average	Test	Average	Test	Average
Room temperature	0.109(0.277)	112(770)		44		47	
		113(780)	112(770)	44	44	39	45
		112(770)		45		49	
	0.063(0.160)	120(830)		39		54	
		119(820)	119(820)	36	38	55	54
		118(810)		38		53	
	0.041(0.104)	120(830)		32		49	
		120(830)	120(830)	33	32	50	53
		119(820)		31		60	

NOTE: (1) Gauge length was 2 in. (5 cm) except that at elevated temperature the gauge length for 0.1-and 0.02-in. (0.03 and 0.05 cm) sheet was about 2.5 in. (6.4 cm).

TABLE I. Concluded

f. AS-RECEIVED WIRE, 10 IN./MIN (0.42 cm/s) CROSSHEAD SPEED AT ELEVATED TEMPERATURES (Continued)

Temperature, °F(°K)	Initial diameter, in.(cm)	Ultimate strength, ksi (MN/m^2)		Elongation, percent		Reduction in area, percent	
		Test	Average	Test	Average	Test	Average
Room temperature	0.020(0.051)	135(930)		21		40	
		136(940)	136(940)	24	23	39	40
		137(940)		24		40	
1340(1000)	0.109(0.277)	73(500)		40		52	
		72(500)	72(500)	42	41	53	53
		72(500)		41		54	
	0.063(0.160)	78(540)		39		58	
		77(530)	78(540)	37	38	58	58
		79(540)		37		59	
	0.041(0.104)	83(570)		35		60	
		84(580)	82(570)	35	36	59	59
		78(540		37		57	
	0.020(0.051)	93(640)		23		33	
		92(630)	92(630)	20	22	46	44
		91(630)		23		54	
1540(1110)	0.109(0.277)	51(350)		70		74	
		54(370)	54(370)	60	62	73	73
		57(390)		57		73	
	0.063(0.160)	57(390)		42		75	
		56(390)	57(390)	41	42	77	75
		57(390)		43		72	
	0.041(0.104)	57(390)		41		73	
		56(390)	56(390)	39	39	70	72
		56(390)		38		73	
	0.020(0.051)	65(450)		27		40	
		65(450)	65(450)	30	30	42	42
		66(460)		32		45	

NOTE: (1) Gauge length was 2 in. (5 cm) except that at elevated temperature the gauge length for 0.01- and 0.02-in. (0.03 and 0.05 cm) sheet was about 2.5 in. (6.4 cm).

TABLE 2

INCONEL 625 SHEET TENSILE TEST RESULTS

a. AS-RECEIVED

Temperature, °F(°K)	Initial dimensions, in.(cm)		Ultimate strength, ksi (MN/m^2)		Yield strength, ksi (MN/m^2)		Elongation, percent		Reduction in area, percent	
	Width	Thickness	Test	Average	Test	Average	Test	Average	Test	Average
Room temperature	0.50(1.3)	0.114(0.290)	137(940)		79(540)		43		41	
			135(930)	136(940)	78(540)	78(540)	44	44	44	43
			136(940)		78(540)		44		44	
	0.50(1.3)	0.066(0.168)	128(880)		67(460)		46		50	
			129(890)	129(890)	68(470)	68(470)	47	46	50	50
			129(890)		68(470)		46		50	
	0.50(1.3)	0.041(0.104)	132(910)		70(480)		49		48	
			132(910)	132(910)	70(480)	70(480)	49	49	48	48
			132(910)		69(480)		49		47	
	0.50(1.3)	0.022(0.056)	133(920)		69(480)		47		47	
			135(930)	134(920)	69(480)	69(480)	47	47	46	47
			134(920)		69(480)		48		47	
	0.50(1.3)	0.008(0.020)	134(920)		64(440)		47		40	
			135(930)	135(930)	66(460)	64(440)	47	48	40	40
			135(930)		64(440)		49		41	
1340(1000)	0.50(1.3)	0.114(0.290)	103(710)		-(2)		49		50	
	.37(.9)		105(720)	105(720)	59(410)	59(410)	45	46	53	48
	.37(.9)		107(740)		59(410)		45		41	
	0.50(1.3)	0.008(0.020)	92(630)		38(260)		51		43	
			95(650)	95(670)	41(280)	40(280)	35	42	33	37
			97(670)		40(280)		41		34	
1540(1110)	0.37(0.9)	0.114(0.290)	79(540)		52(360)		57		73	
	.35(.9)		79(540)		52(360)		53		71	
	.35(.9)		77(530)	79(540)	51(350)	52(360)	55	53	77	73
	.37(.9)		78(540)		51(350)		51		74	
	.37(.9)		80(550)		53(370)		40		68	
	0.50(1.3)	0.008(0.020)	75(520)		43(300)		51		47	
			74(510)	75(520)	43(300)	43(300)	53	54	50	49
			75(520)		43(300)		57		51	

NOTES: (1) Gauge length was 2 in. (5 cm) except that at elevated temperature the gauge length for 0.01- and 0.02-in. (0.03 and 0.05 cm) sheet was about 2.5 in. (6.4 cm).

(2) Extensometer grips moved during test.

TABLE 2. Continued

b. AS-RECEIVED WITH 1925°F(1330°K) SOAK FOR 300 SECONDS

Temperature, °F(°K)	Initial dimensions, in.(cm)		Ultimate strength, ksi (MN/m^2)		Yield strength, ksi (MN/m^2)		Elongation, percent		Reduction in area, percent	
	Width	Thickness	Test	Average	Test	Average	Test	Average	Test	Average
Room temperature	0.50(1.3)	0.114(0.290)	126(860)		58(400)		49		45	
			127(870)	127(870)	59(410)	59(410)	49	49	48	47
			128(880)		60(410)		48		48	
1340(1000)	0.50(1.3)	0.114(0.290)	97(670)		41(280)		53		47	
			97(670)	97(670)	40(280)	40(280)	55	55	48	48
			97(670)		39(270)		56		48	
1540(1110)	0.50(1.3)	0.114(0.290)	75(520)		38(260)		61		67	
			74(510)		-(2)		53		64	
			77(530)	75(520)	40(280)	39(270)	56	59	66	67
			75(520)		38(260)		64		69	
			75(520)		39(270)		58		67	
			75(520)		39(270)		61		68	

NOTES: (1) Gauge length was 2 in. (5 cm) except that at elevated temperature the gauge length for 0.01- and 0.02-in. (0.03 and 0.05 cm) sheet was about 2.5 in. (6.4 cm).
(2) Estensometer grips moved during test.

c. COATED WITH PALNIRO I

Temperature, °F(°K)	Initial dimensions, in.(cm)		Ultimate strength, ksi (MN/m^2)		Yield strength, ksi (MN/m^2)		Elongation, percent		Reduction in area, percent	
	Width	Thickness	Test	Average	Test	Average	Test	Average	Test	Average
Room temperature	0.5(1.3)	0.009(0.023)	125(860)		59(410)		44		38	
			124(850)	124(850)	59(410)	59(410)	40	43	34	37
			124(850)		59(410)		44		38	
1340(1000)	0.5(1.3)	0.009(0.023)	84(580)		39(270)		33		28	
			81(560)	83(570)	38(260)	38(260)	27	31	25	28
			84(580)		38(260)		32		30	
1540(1110)	0.5(1.3)	0.009(0.023)	64(440)		34(230)		22		22	
			66(460)	66(460)	35(240)	35(240)	27	26	27	25
			67(460)		35(240)		28		26	

NOTE: (1) Gauge length was 2 in. (5 cm) except that at elevated temperature the gauge length for 0.01- and 0.02-in. (0.03 and 0.05 cm) sheet was about 2.5 in. (6.4 cm).

TABLE 2. Concluded

d. COATED WITH PALNIRO 7

Temperature °F(°K)	Initial dimensions, in. (cm)		Ultimate strength, ksi (MN/m^2)		Yield strength, ksi (MN/m^2)		Elongation, percent		Reduction in area, percent	
	Width	Thickness	Test	Average	Test	Average	Test	Average	Test	Average
Room temperature	0.50(1.3)	0.009(0.023)	129(880)		63(430)		45		40	
			130(900)	130(900)	64(440)	64(440)	44	44	40	40
			130(900)		65(450)		43		41	
1340(1000)	0.50(1.3)	0.009(0.023)	91(630)		41(280)		41		33	
			91(630)	91(630)	41(280)	41(280)	41	40	32	31
			92(630)		41(280)		39		29	
1540(1000)	0.50(1.3)	0.009(0.023)	70(480)		38(260)		46		40	
			70(480)	70(480)	38(260)	38(260)	56	49	41	40
			70(480)		39(270)		45		39	

NOTE: (1) Gauge length was 2 in. (5 cm) except that at elevated temperature the gauge length for 0.01- and 0.02-in. (0.03 and 0.05 cm) sheet was about 2.5 in. (6.4 cm).

TABLE 3

INCONEL X-750 SHEET
TENSILE TEST RESULTS

Condition	Test temperature, °F (°K)	Ultimate strength, ksi (MN/m^2)		Yield strength, ksi (MN/m^2)		Elongation, percent		Reduction in area, percent	
		Test	Average	Test	Average	Test	Average	Test	Average
As-received plus Palniro 1 coating	Room temperature	155(1070)	155(1070)	101(700)	101(700)	18	18	27	27
	1340(1000)	117(810)	117(810)	88(610)	88(610)	7	7	16	16
	1540(1110)	---(1)	---	59(410)	59(410)	1	1	8	8
As-received plus Palniro 7 coating	Room temperature	163(1120) 163(1120) 165(1140)	164(1130)	102(700) 100(690) 104(720)	102(700)	27 30 28	28	32 33 32	32
	1340(1000)	123(850)	123(850)	88(610)	88(610)	9	9	15	15
	1540(1110)	---(1)	---	61(420)	61(420)	5	5	13	13

NOTES: (1) Fracture occurred on the reloading cycle prior to reaching engineering ultimate.
(2) Initial specimen dimensions; 0.50 in. (1.3 cm) width, 0.011 in. (0.028 cm) thickness.
(3) Gauge length was 2 in. (5 cm) except that at elevated temperature the gauge length for 0.01- and 0.02-in. (0.03 and 0.05 cm) sheet was about 2.5 in. (6.4 cm).

TABLE 4

PARENT METAL FATIGUE RESULTS

a. HASTELLOY X

Fracture depth, in. (cm)	Surface condition	Test temperature, °F (°K)	5-in. (13 cm) mandrel			9-in. (23 cm) mandrel			16-in. (41 cm) mandrel		
			h/h_o	Cycles		h/h_o	Cycles		h/h_o	Cycles	
				Test	Average		Test	Average		Test	Average
0.01(0.03)	Polished externally	Room temperature	1.017	65		1.013	228		1.017	1600	
			1.017	59	73	1.013	350		1.017	1610	1580
			1.017	74		1.017	390	352	1.021	1260	
			1.017	90		1.017	455		1.021	2060	
						1.021	276				
						1.021	398				
		1340(1000)	1.017	30		1.008	77		0.996	180	
			1.017	34	31	1.013	75	78	1.000	138	162
			1.017	25		1.013	77		1.000	172	
			1.017	31							
		1540(1110)	1.025	21		1.008	53		1.004	120	
			1.025	25	24	1.008	60	56	1.000	119	123
			1.021	25		1.017	50		1.000	130	
			1.021	23		1.017	54				
	Polished internally and externally	Room temperature	1.013	96					1.017	1585	
			1.013	108	105				1.017	1659	1890
			1.013	97					1.008	2367	
			1.013	108							
		1540(1110)							1.017	97	106(1)
									1.017	109	
									1.021	140	139(2)
									1.021	128	
0.24(0.61)	30 to 60 μin. (0.8 to 1.5 μm) finish	Room temperature	0.979	136	130	0.975	517	516	0.992	2975	2900
			.983	134		.992	508		.996	2904	
			.996	131		.992	566		.983	2989	
		1340(1000)	0.975	48	47	0.983	128	131	0.983	379	378
			.983	79		.983	147		.983	385	
			.983	31		.983	132		.983	410	
		1540(1110)	0.983	43	43	0.983	108	99	0.975	224	270
			.979	41		.983	120		.983	228	
			.983	50		.983	83		.979	471	

NOTES: (1) 0.017 Hz tests
(2) 0.10 Hz tests
(3) Strain ranges are listed in table 8.
(4) Cavity specimen (0.01-in. (0.03 cm) fracture depth) was brazed at 1950°F (1340°K) for 300 s with Palniro 7 (70 Au, 8 Pd, 22 Ni).

TABLE 4. Concluded

b. INCONEL 625

Fracture depth, in. (cm)	Surface condition	Test temperature, °F (°K)	5-in. (13 cm) mandrel			9-in. (23 cm) mandrel			16-in. (41 cm) mandrel		
			h/h_o	Cycles		h/h_o	Cycles		h/h_o	Cycles	
				Test	Average		Test	Average		Test	Average
0.01(0.03)	Polished externally	Room temperature	1.017	130		1.017	572		1.021	2836	
			1.017	100	108	1.017	614	609	1.021	2940	3160
			1.017	85		1.017	631		1.025	3070	
			1.017	110		1.017	545		1.025	3250	
		1340(1000)	1.021	21		1.017	77		1.017	181	
			1.021	22	23	1.017	79	80	1.013	210	227
			1.021	23		1.017	75		1.021	228	
			1.021	23		1.017	78		1.021	266	
		1540(1110)	1.021	19					1.025	102	
			1.021	21	17				1.025	125	120
			1.017	14					1.008	116	
			1.017	12					1.008	125	
	Polished internally and externally	Room temperature							1.025	3245	
									1.025	3190	3500
									1.021	3586	
									1.021	3457	
0.24(0.61)	30 to 60 μin. (0.8 to 1.5 μm) finish	Room temperature	0.996	123	115	0.983	391	427	0.996	3309	3100
			1.000	115		.958	463		.996	3063	
			1.021	103		.996	490		.992	3049	
		1340(1000)	0.983	53	58	0.983	153	155	0.983	446	475
			.983	60		.979	161		.983	463	
			.979	70		.983	170		.979	575	
		1540(1110)	0.979	66	55	0.983	131	125	0.896	335	264
			.983	61		.975	140		.896	292	
			.983	46		.983	120		.892	370	

NOTES: (3) Strain ranges are listed in table 8.
(4) Cavity specimen (0.01-in. (0.03 cm) fracture depth) was brazed at 1950°F(1340°K) for 300 s with Palniro 7 (70 Au, 8 Pd, 22 Ni).

TABLE 5

SUMMARY OF RELATIONS FOR COMPUTING FATIGUE LIFE

Investigator	Reference (see text)	C	c
Coffin	6	$0.5\ \varepsilon_f$	2.0
Manson	7	$\varepsilon_f^{0.75}$	1.7
	6	$0.8\ \varepsilon_f^{0.75}$	2.0
	3	$\varepsilon_f^{0.6}$	1.7
Martin	8	$0.7\ \varepsilon_f$	2.0
Morrow	9	$1.3\ \varepsilon_f$	1.7

NOTE: $\varepsilon_f = \ln [100/(100-RA)]$

TABLE 6

PLATE-FIN FATIGUE RESULTS

a. HASTELLOY X

Braze alloy	Temperature, °F (°K)	5-in. (13 cm) mandrel			9-in. (23 cm) mandrel			16-in. (41 cm) mandrel			32-in. (81 cm) mandrel		
		h/h_o	Cycles		h/h_o	Cycles		h/h_o	Cycles		h/h_o	Cycles	
			Test	Average		Test	Average		Test	Average		Test	Average
Palniro 1	Room temperature	1.000	11	10	0.996	43	45	0.996	207	230			
		1.000	11		.996	54		.996	216				
		.996	10		.992	41		.996	233				
		.996	7		.992	56		.996	275				
					.992	44							
					.992	40							
	1340(1000)				1.000	24	20	0.992	41	57	0.996	440	517
					1.000	22		.992	55		.996	539	
					1.000	15		1.000	41		.988	504	
					1.000	18		1.000	56		.988	647	
					.992	14		1.008	48				
					.992	20		.996	93				
					1.000	25		.996	94				
					1.000	24							
	1540(1110)				1.000	16	15	0.988	63	47	0.992	233	248
					1.000	17		.988	64		.992	240	
					1.000	12		.996	38		.979	294	
					1.000	28		.996	43				
					.992	10		1.004	48				
					.992	10		1.004	49				
					.996	16		.996	50				
					.996	19		.996	56				
					.992	14							
					.992	14							
Palniro 1	1540(1110), 200 s hold time				0.996	10	11	1.000	34	33	0.988	113	98
					1.004	10		1.000	30		.988	104	
					1.000	14		1.000	34		.988	91	
					1.000	17		1.000	36		.988	93	
					.992	8							
					.992	7							
Palniro 7	Room temperature	1.000	7	7	1.000	25	26	1.000	175	176			
					1.000	27		1.000	177				
	1540(1110)				1.004	22	16	0.996	61	55	0.988	240	219
					1.000	16		1.000	51		.988	225	
					1.000	16		1.000	53		.988	211	
					1.004	13					.988	224	
					1.004	14							

NOTES: (1) Strain ranges are given in table 8.
(2) Palniro 1 (50 Au, 25 Pd, 25 Ni) was brazed at 2070°F (1410°K) and Palniro 7 (70 Au, 8 Pd, 22 Ni) was brazed at 1950°F (1340°K), time at braze temperature was 1200 s.

TABLE 6. Concluded

b. INCONEL 625

Braze alloy	Temperature, °F (°K)	5-in. (13 cm) mandrel			9-in. (23 cm) mandrel			16-in. (41 cm) mandrel			32-in. (81 cm) mandrel		
		h/h_o	Cycles		h/h_o	Cycles		h/h_o	Cycles		h/h_o	Cycles	
			Test	Average		Test	Average		Test	Average		Test	Average
Palniro 1	Room temperature	1.000	7	8	1.000	31	29	1.000	87	116			
		1.000	9		1.000	31		1.000	113				
		.996	7		1.000	25		1.004	146				
		.996	8		1.000	27		1.004	151				
					1.004	29		.992	93				
					1.004	31		.992	122				
	1340(1000)				1.000	8	9	0.996	34	35	0.988	656	713
					1.000	10		.996	39		.988	779	
					1.000	9		1.000	36		.983	741	
					1.000	10		1.000	22		.983	767	
								1.000	36				
								1.000	46				
	1540(1110)				1.021	10	12	1.004	42	27	1.000	175	180
					1.021	11		1.004	44		1.000	180	
					1.000	13		1.000	18		1.000	169	
					1.000	14		1.000	18		1.000	197	
								.992	28				
								.992	22				
Palniro 7	Room temperature	1.013	12	13	1.000	46	48	1.004	159	169			
		1.013	14		1.000	50		1.004	176				
	1540(1100)				1.004	17	17	1.008	43	47	1.000	221	193
					1.004	18		1.008	49		1.000	182	
											1.000	202	
											.996	178	
											.996	186	

c. FINS ORIENTED 90 DEGREES (INCONEL X-750 SHEETS, INCONEL 625 FINS)

Braze alloy	Temperature, °F (°K)	9-in. (23 cm) mandrel			16-in. (41 cm) mandrel		
		h/h_o	Cycles		h/h_o	Cycles	
			Test	Average		Test	Average
Palniro 7	Room temperature	1.000	160	161	1.004	535	581
		1.000	163		1.004	560	
					.996	580	
					.996	658	
	1540(1110)	1.008	2	2	1.004	5	5
		1.008	3		1.004	6	

NOTES: (1) Strain ranges are given in table 8.
(2) Palniro 1 (50 Au, 25 Pd, 25 Ni) was brazed at 2070°F (1410°K) and Palniro 7 (70 Au, 8 Pd, 22 Ni) was brazed at 1950°F (1340°K), time at braze temperature was 1200 s.

TABLE 7

TYPICAL REDUCTION IN AREA MEASUREMENTS
(As-Received Hastelloy X Sheet at 1540°F (1110°K))

a. U. S. CUSTOMARY UNITS

Initial thickness, in.	Final thickness, in.						Final width, in.	Average final area, $in.^2$	Initial area, $in.^2$	Reduction in area, percent
	Thicknesses 0.01 to 0.02 in. from both sides of the fracture at five points across the width					Average				
	1	2	3	4	5					
0.113	0.0861 .0908	0.0844 .0880	0.0812 .0872	0.0833 .0858	0.0868 .0865	0.0860	0.335	0.0288	0.0489	41
0.113	0.0840 .0850	0.0829 .0844	0.0822 .0842	0.0824 .0824	0.0860 .0850	0.0839	0.322	0.0270	0.0481	45
0.113	0.0864 .0874	0.0829 .0854	0.0829 .0852	0.0854 .0854	0.0863 .0860	0.0853	0.381	0.0325	0.0566	43
0.063	0.0417 .0424	0.0394 .0386	0.0377 .0378	0.0394 .0371	0.0411 .0409	0.0396	0.347	0.0137	0.0316	57
0.063	0.0434 .0414	0.0394 .0391	0.0404 .0414	0.0413 .0414	0.0426 .0412	0.0406	0.354	0.0144	0.0316	55
0.063	0.0382 .0419	0.0397 .0400	0.0396 .0382	0.0398 .0388	0.0390 .0408	0.0396	0.349	0.0138	0.0316	56
0.043	0.0319 .0296	0.0299 .0293	0.0280 .0268	0.0284 .0291	0.0300 .0292	0.0292	0.367	0.0107	0.0211	49
0.043	0.0287 .0297	0.0290 .0279	0.0284 .0280	0.0290 .0274	0.0306 .0281	0.0287	0.361	0.0104	0.0211	51
0.042	0.0272 .0278	0.0271 .0284	0.0280 .0267	0.0280 .0283	0.0280 .0290	0.0278	0.360	0.0101	0.0208	51
0.023	0.0161 .0171	0.0166 .0169	0.0152 .0144	0.0166 .0144	0.0155 .0160	0.0159	0.379	0.0060	0.0115	48
0.023	0.0160 .0164	0.0163 .0160	0.0161 .0154	0.0163 .0148	0.0161 .0160	0.0159	0.369	0.0059	0.0115	49
0.023	0.0161 .0162	0.0166 .0161	0.0163 .0158	0.0151 .0155	0.0162 .0158	0.0160	0.371	0.0059	0.0115	49
0.010	0.0073 .0072	0.0072 .0073	0.0074 .0076	0.0076 .0071	0.0072 .0070	0.0073	0.399	0.0029	0.0051	43
0.010	0.0080 .0079	0.0080 .0079	0.0079 .0078	0.0077 .0082	0.0078 .0082	0.0079	0.403	0.0032	0.0051	37
0.010	0.0082 .0078	0.0077 .0077	0.0078 .0080	0.0080 .0082	0.0077 .0076	0.0079	0.397	0.0031	0.0051	39

TABLE 7. Concluded

b. SI UNITS

Initial thickness, cm	Final thickness, cm						Final width, cm	Average final area, cm^2	Initial area, cm^2	Reduction in area, percent
	Thicknesses 0.03 to 0.05 cm from both sides of the fracture at five points across the width					Average				
	1	2	3	4	5					
0.287	0.219 .231	0.214 .224	0.206 .221	0.212 .218	0.220 .220	0.218	0.850	0.0732	0.1242	41
0.287	0.213 .216	0.211 .214	0.209 .214	0.209 .209	0.218 .216	0.213	0.818	0.0686	0.1222	45
0.287	0.219 .222	0.211 .217	0.211 .216	0.217 .217	0.219 .218	0.217	0.968	0.0826	0.1438	43
0.160	0.106 .108	0.100 .098	0.096 .096	0.100 .094	0.104 .104	0.101	0.881	0.0348	0.0803	57
0.160	0.110 .105	0.100 .099	0.103 .105	0.105 .105	0.108 .105	0.103	0.899	0.0366	0.0803	55
0.160	0.097 .106	0.101 .102	0.101 .097	0.101 .099	0.099 .104	0.101	0.886	0.0351	0.0803	56
0.109	0.081 .075	0.076 .074	0.071 .068	0.072 .074	0.076 .074	0.074	0.932	0.0272	0.0536	49
0.109	0.073 .075	0.074 .071	0.072 .071	0.074 .070	0.078 .071	0.073	0.917	0.0264	0.0536	51
0.109	0.069 .071	0.069 .072	0.071 .068	0.071 .072	0.071 .074	0.071	0.914	0.0257	0.0528	51
0.058	0.041 .043	0.042 .043	0.039 .037	0.042 .037	0.039 .041	0.040	0.963	0.0152	0.0292	48
0.058	0.041 .042	0.041 .041	0.041 .039	0.041 .038	0.041 .041	0.040	0.937	0.0150	0.0292	49
0.058	0.041 .041	0.042 .041	0.041 .040	0.038 .039	0.041 .040	0.041	0.942	0.0150	0.0292	49
0.025	0.019 .018	0.018 .019	0.019 .019	0.019 .018	0.018 .018	0.019	1.013	0.0074	0.0130	43
0.025	0.020 .020	0.020 .020	0.020 .020	0.020 .020	0.020 .021	0.020	1.024	0.0081	0.0130	37
0.025	0.021 .020	0.020 .020	0.020 .020	0.020 .020	0.020 .021	0.020	1.008	0.0079	0.0130	39

TABLE 8

PLASTIC STRAIN RANGES

a. 1925°F (1330°K) CYCLE, 0.11-IN. (0.28 cm) SHEET(CAVITY PARENT METAL SPECIMENS)

Mandrel radius		Applied total engineering strain, ϵ_l', percent	Total true strain ϵ_l, percent	True plastic strain range, percent					
				Hastelloy X			Inconel 625		
in.	cm			80°F (300°K)	1340°F (1000°K)	1540°F (1110°K)	80°F (300°K)	1340°F (1000°K)	1540°F (1110°K)
5	13	4.69	4.58	3.81	3.85	3.97	3.79	3.80	3.94
9	23	2.63	2.60	1.91	1.95	2.05	1.89	1.90	2.02
16	41	1.49	1.48	.87	.90	.99	.85	.87	.97

b. AS-RECEIVED, 0.11-IN. (0.28 cm) SHEET (SOLID PARENT METAL SPECIMENS)

Mandrel radius		Applied total engineering strain, ϵ_l', percent	Total true strain component ϵ_l, percent	True equivalent plastic strain range, percent					
				Hastelloy X			Inconel 625		
in.	cm			80°F (300°K)	1340°F (1000°K)	1540°F (1110°K)	80°F (300°K)	1340°F (1000°K)	1540°F (1110°K)
5	13	4.69	4.58	4.43	4.51	4.60	4.27	4.30	4.48
9	23	2.63	2.60	2.23	2.31	2.38	2.10	2.12	2.28
16	41	1.49	1.48	1.03	1.09	1.16	.92	.93	1.07

c. PALNIRO I COATING, 0.01-IN. (0.03 cm) SHEET

Mandrel radius		Applied total engineering strain, ϵ_l', percent	Total true strain component, ϵ_l, percent	True equivalent plastic strain range, percent					
				Hastelloy X			Inconel 625		
in.	cm			80°F (300°K)	1340°F (1000°K)	1540°F (1110°K)	80°F (300°K)	1340°F (1000°K)	1540°F (1110°K)
5	13	4.69	4.58	4.33	4.44	4.63	4.36	4.49	4.61
9	23	2.63	2.60	2.15	2.24	2.41	2.17	2.24	2.39
16	41	1.49	1.48	.96	1.04	1.18	.98	1.07	1.17
32	81	.75	.74	.26	.31	.42	.27	.33	.40

d. PALNIRO 7 COATING, 0.01-IN. (0.03 cm) SHEET

Mandrel radius		Applied total engineering strain, ϵ_l', percent	Total true strain component ϵ_l, percent	True equivalent plastic strain range, percent				
				Hastelloy X		Inconel 625		Inconel X-750
in.	cm			80°F (300°K)	1540°F (1110°K)	80°F (300°K)	1540°F (1110°K)	80°F (300°K)
5	13	4.69	4.58	4.32	4.61	4.31	4.57	4.12
9	23	2.63	2.60	2.14	2.39	2.13	2.36	1.96
16	41	1.49	1.48	.95	1.17	.94	1.14	.80
32	81	.75	.74	.25	.41	.24	.38	.16

TABLE 9

MATERIAL PROPERTIES

a. TENSILE STRENGTH

Specimen	Material condition	Material	Temperature, °F (°K)	Measured tensile strength, ksi (MN/m^2)		Yield for assumed 0.16 strain hardening exponent, ksi (MN/m^2)	Reduction in area, percent
				Ultimate	Yield		
Parent metal, 0.01 in. (0.03 cm) fracture depth	1925°F (1330°K) cycle, 0.11 in. (0.28 cm) sheet	Hastelloy X	80(300)	118(810)	55(380)	69(480)	41
			1340(1000)	84(580)	36(250)	49(340)	38
			1540(1110)	66(460)	34(230)	38(260)	48
		Inconel 625	80(300)	127(870)	59(410)	74(510)	47
			1340(1000)	97(670)	40(280)	57(390)	48
			1540(1110)	75(520)	39(270)	44(300)	67
Parent metal, 0.24 in. (0.61 cm) fracture depth	As received, 0.11 in. (0.28 cm) sheet	Hastelloy X	80(300)	109(750)	54(370)	64(440)	53
			1340(1000)	73(500)	36(250)	43(300)	43
			1540(1110)	62(430)	35(240)	36(250)	43
		Inconel 625	80(300)	136(940)	78(540)	79(540)	43
			1340(1000)	105(720)	59(410)	61(420)	48
			1540(1110)	79(540)	52(360)	46(320)	73
Plate fin, Palniro 1	Palniro 1 coating, 0.01 in. (0.03 cm) sheet	Hastelloy X	80(300)	122(840)	58(400)	71(490)	33
			1340(1000)	80(550)	34(230)	47(320)	24
			1540(1110)	59(410)	29(200)	34(230)	29
		Inconel 625	80(300)	124(850)	59(410)	72(500)	37
			1340(1000)	83(570)	38(260)	48(330)	28
			1540(1110)	66(460)	35(240)	38(260)	25
Plate-fin, Palniro 7	Palniro 7 coating, 0.01 in. (0.03 cm) sheet	Hastelloy X	80(300)	123(850)	56(390)	72(500)	35
			1540(1110)	60(410)	29(200)	35(240)	35
		Inconel 625	80(300)	130(900)	64(440)	76(520)	40
			1540(1110)	70(480)	38(260)	41(280)	40
		Inconel X-750	80(300)	164(1130)	102(700)	96(660)	32

b. ELASTIC MODULUS

Material	Poisson's ratio (elastic)	Elastic modulus, 10^3 ksi (10^3 MN/m^2)		
		80°F (300°K)	1340°F (1000°K)	1540°F (1110°K)
Hastelloy X	0.3	28.6(197)	21.5(148)	20.3(140)
Inconel 625	.3	29.8(205)	23.5(162)	22.1(152
Inconel X-750	.3	31.0(214)	-	-

c. HASTELLOY X CREEP PROPERTIES

Temperature, °F (°K)	ℓ	A, $(ksi)^{\ell}$-sec $\left[(MN/m^2)^{\ell}\text{-}s\right]$	F, $(ksi)^{-\ell}$-sec^{-1} $\left[(MN/m^2)^{-\ell}\text{-}s^{-1}\right]$
1340(1000)	7.45	1.32×10^{16} (2.32×10^{22})	8.22×10^{-18} (4.67×10^{-24})
1440(1060)	6.88	1.29×10^{14} (7.57×10^{19})	6.66×10^{-16} (1.13×10^{-21})
1540(1110)	6.50	3.34×10^{12} (9.42×10^{17})	2.28×10^{-14} (8.09×10^{-20})

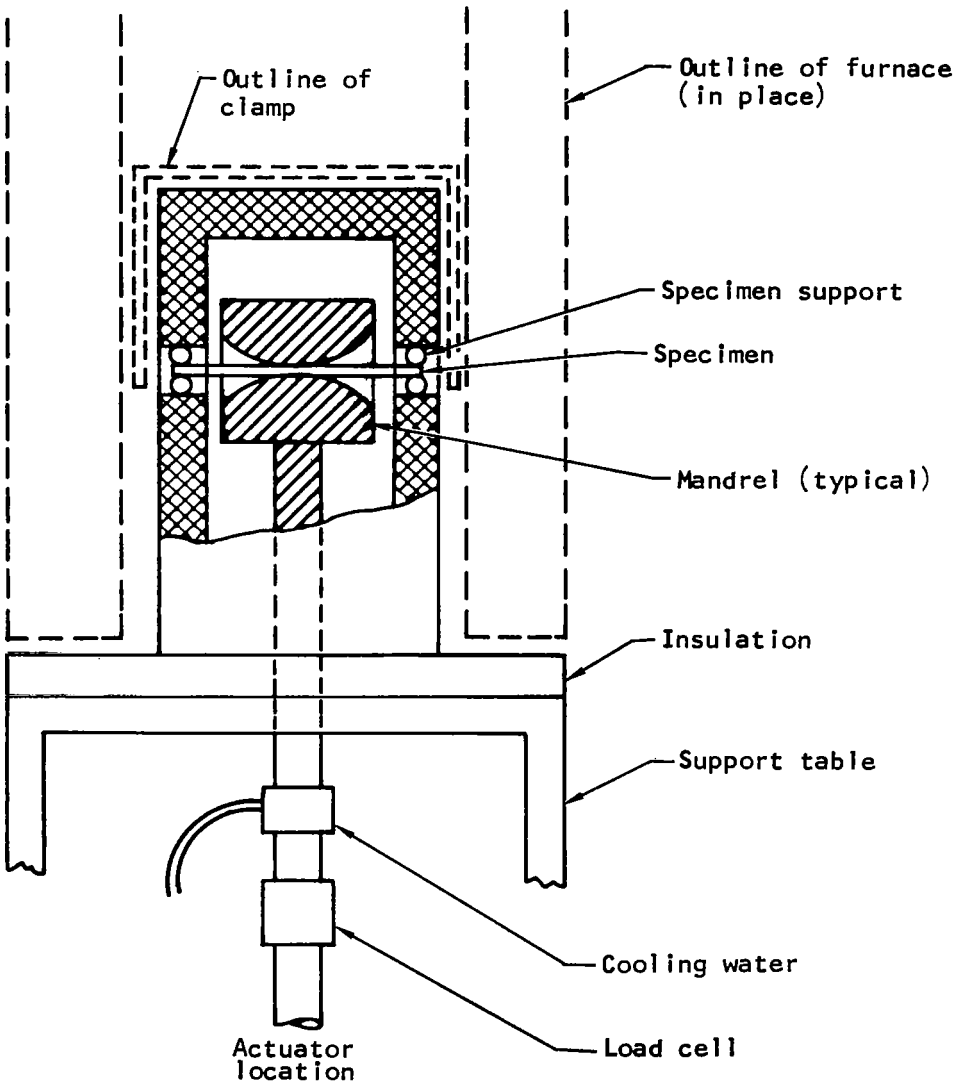

a. Specimen loading and support

Figure 1. Fatique Test Apparatus

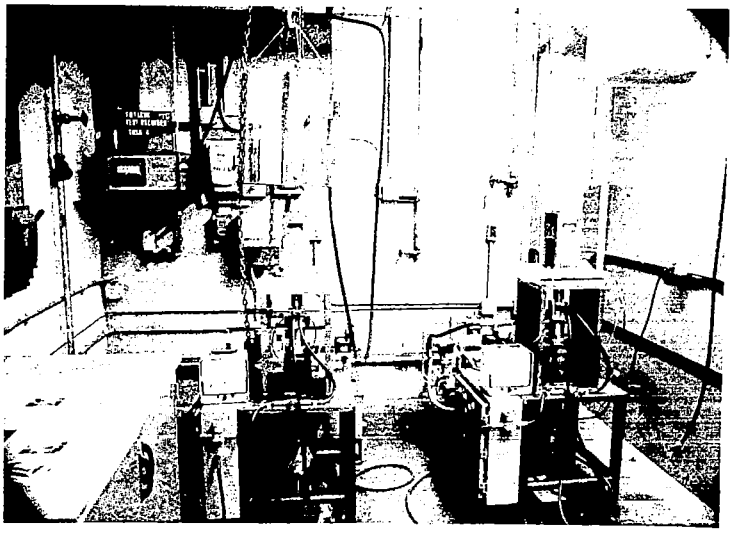

b. Test facility

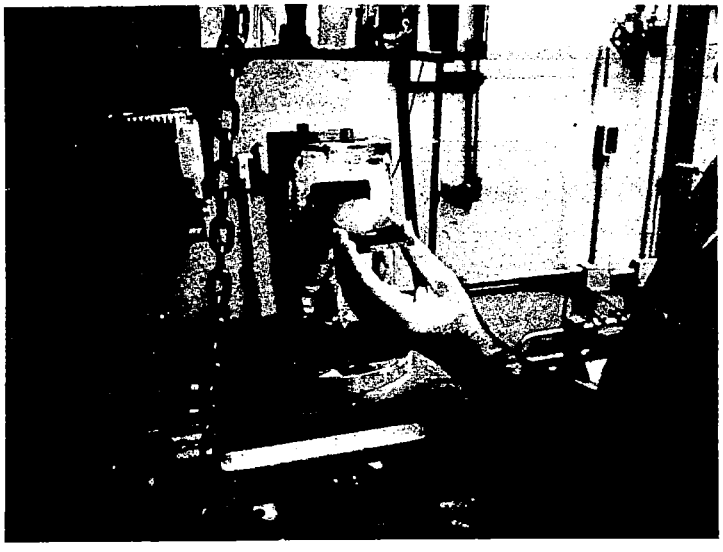

c. Specimen placement in test rig

Figure 1. Concluded

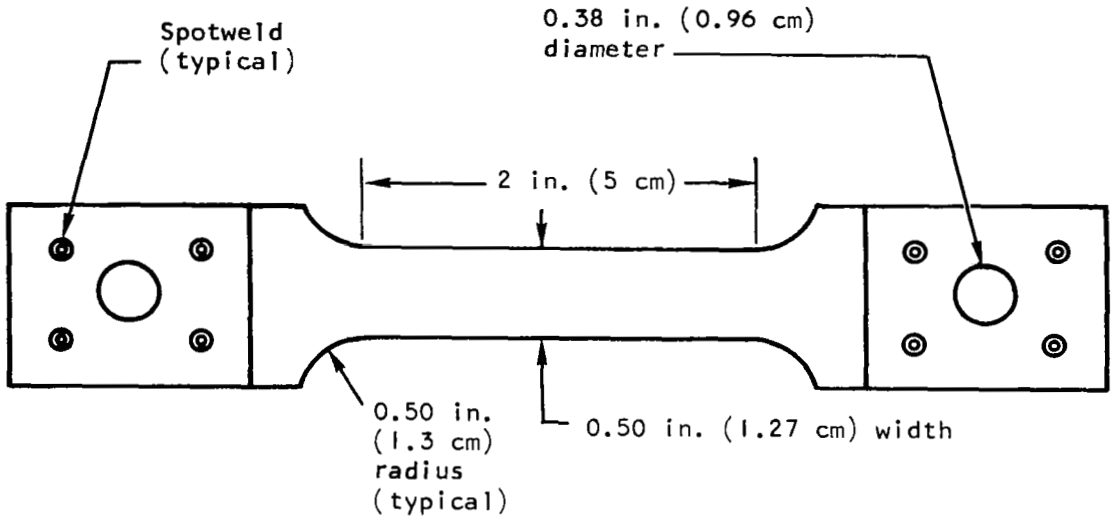

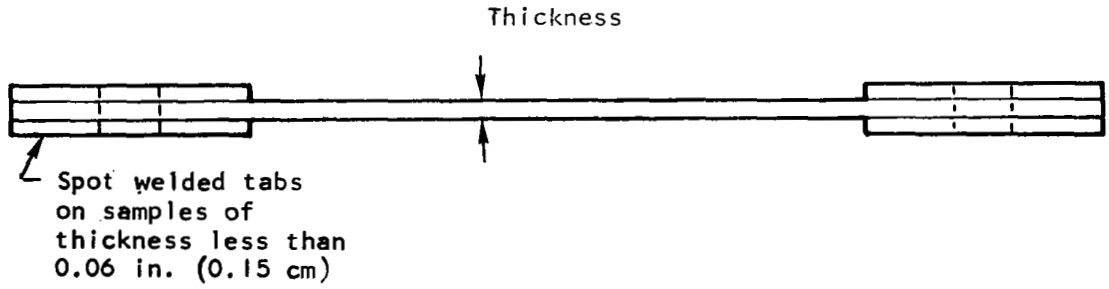

Figure 2. Sheet Tensile Test Specimen

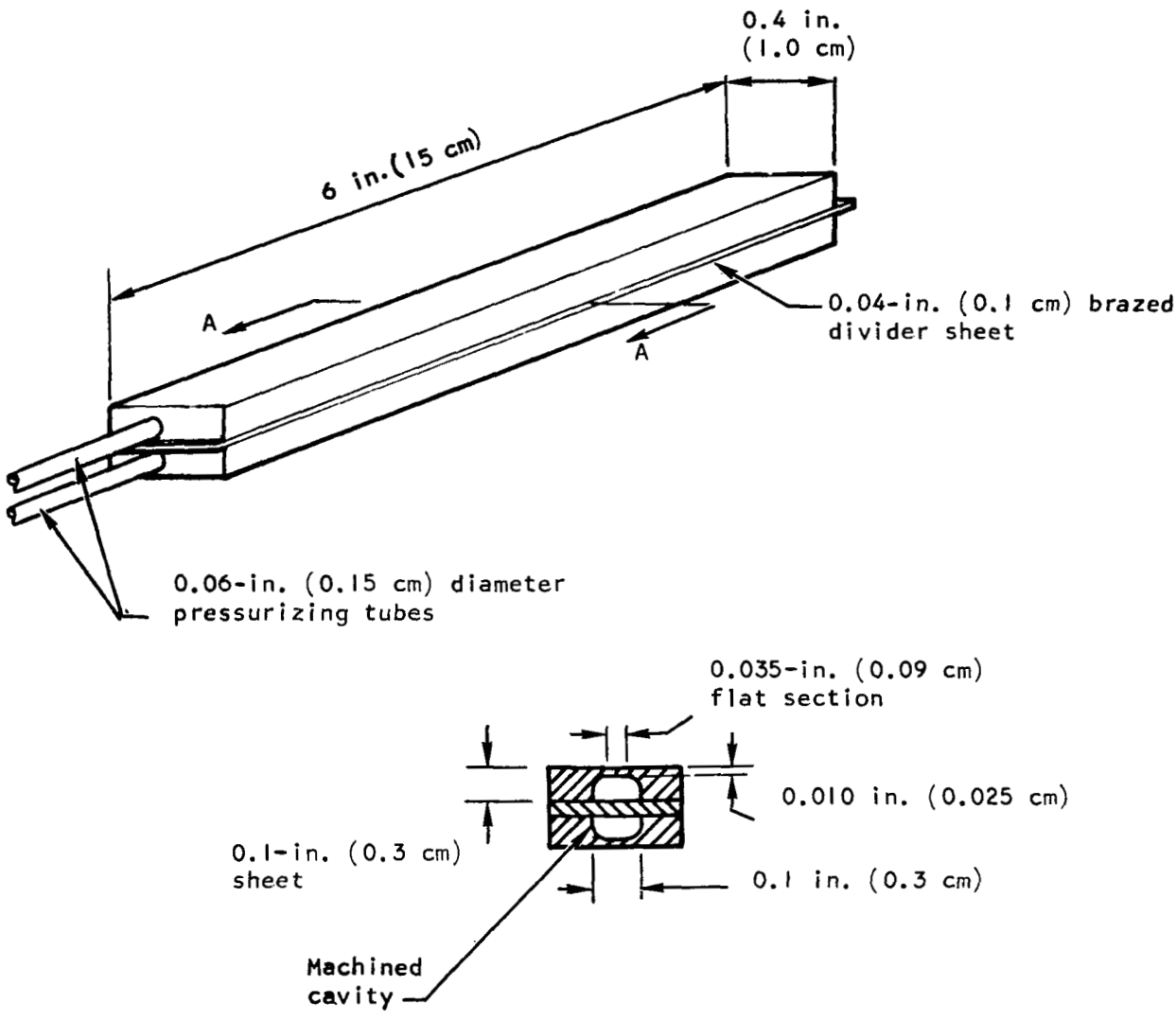

a. Cavity Specimen(Brazed at 1925°F (1330°K) for 300 s)

Figure 3. Parent Metal Fatigue Specimen

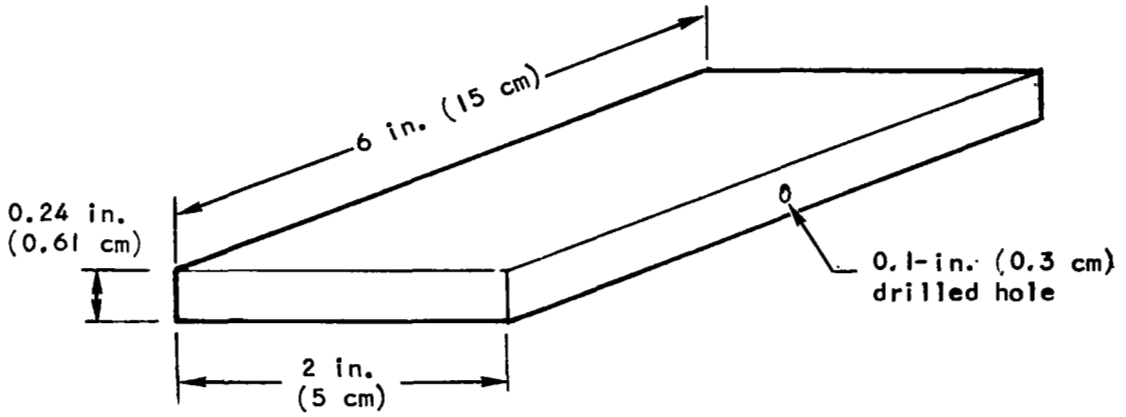

b. Solid Rectangular

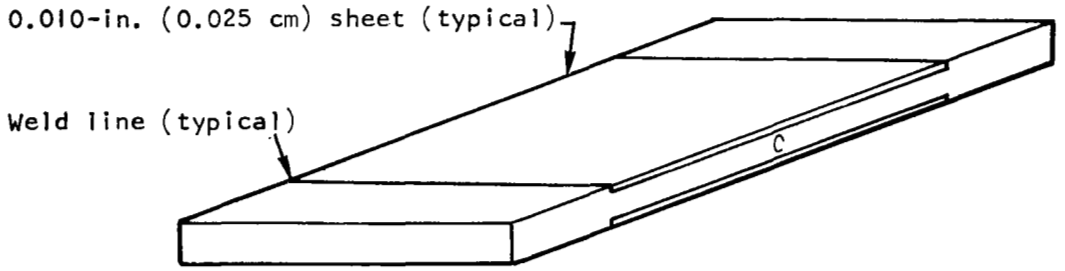

c. Solid Rectangular with Sheet Inserts

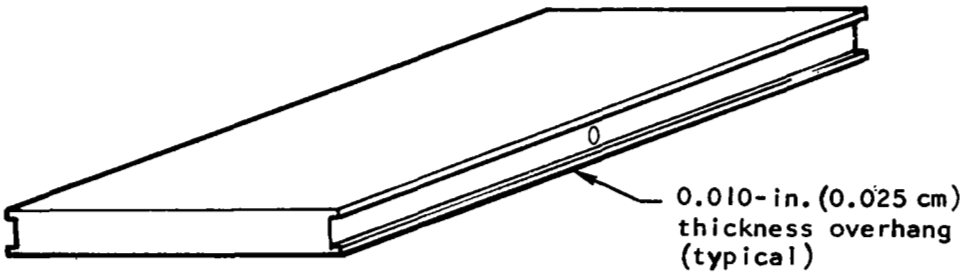

d. Solid Rectangular with Overhangs

Figure 3. Concluded

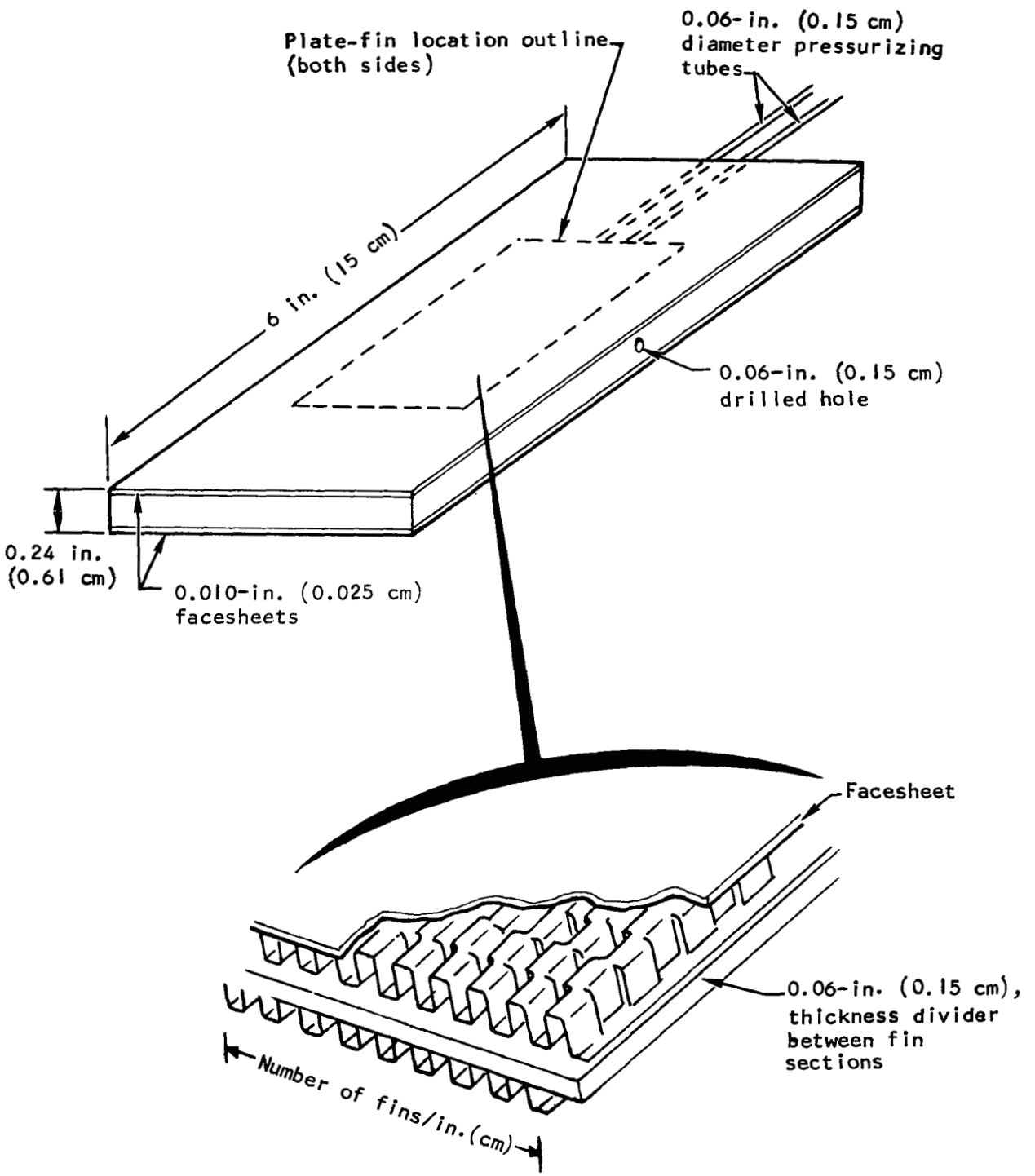

Plate-fin geometry(standard orientation)

Figure 4. Plate-Fin Fatigue Specimen

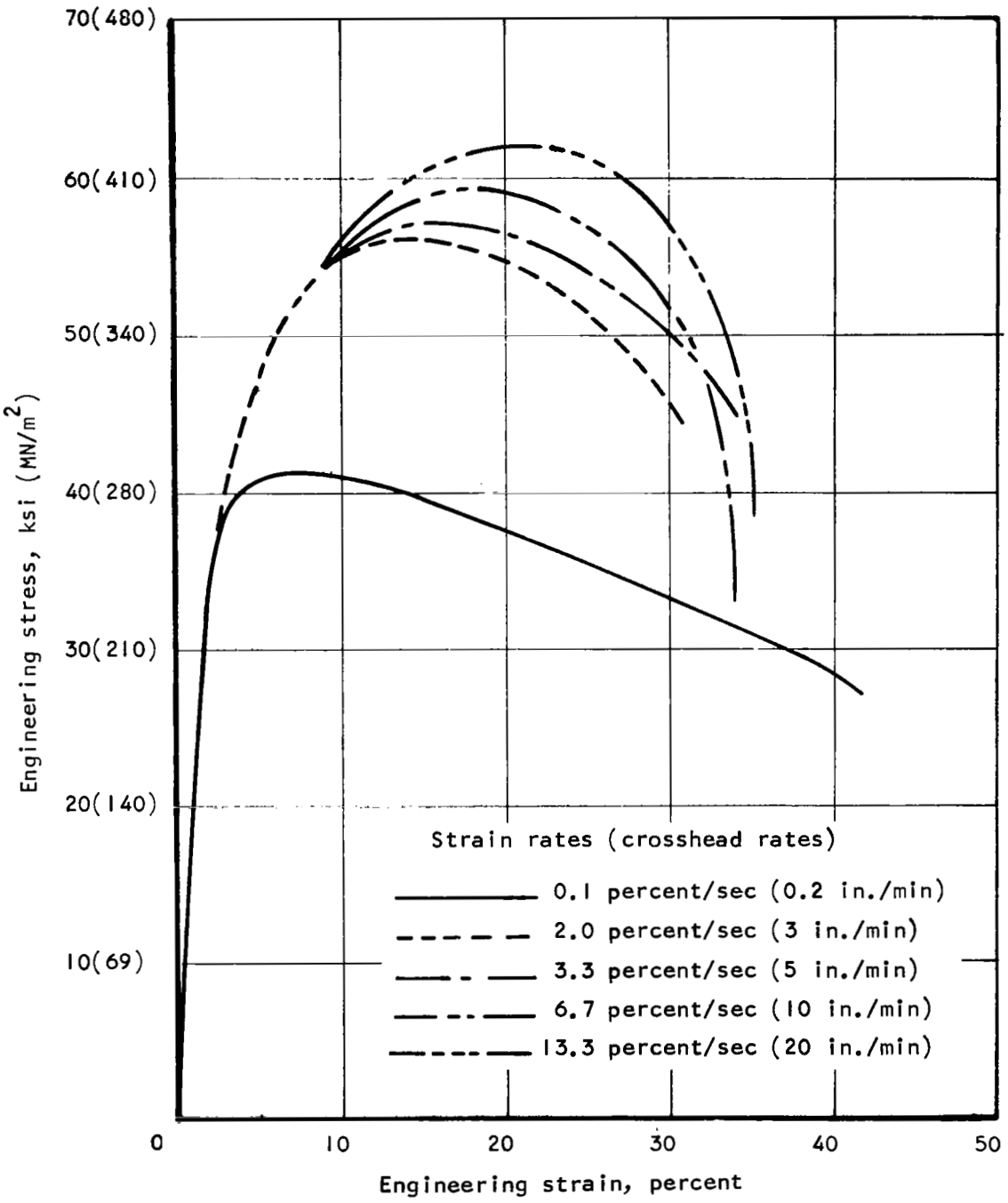

Figure 5. Hastelloy X Stress-Strain Curves vs Strain Rate for 0.01 in. (0.03 cm) Sheet at 1540°F(1110°K)

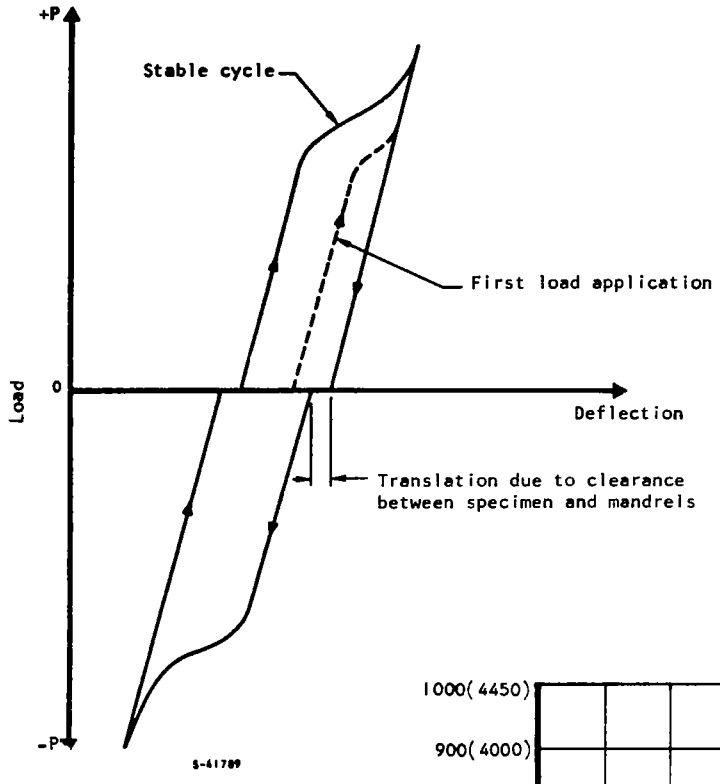

a. Cycle Schematic

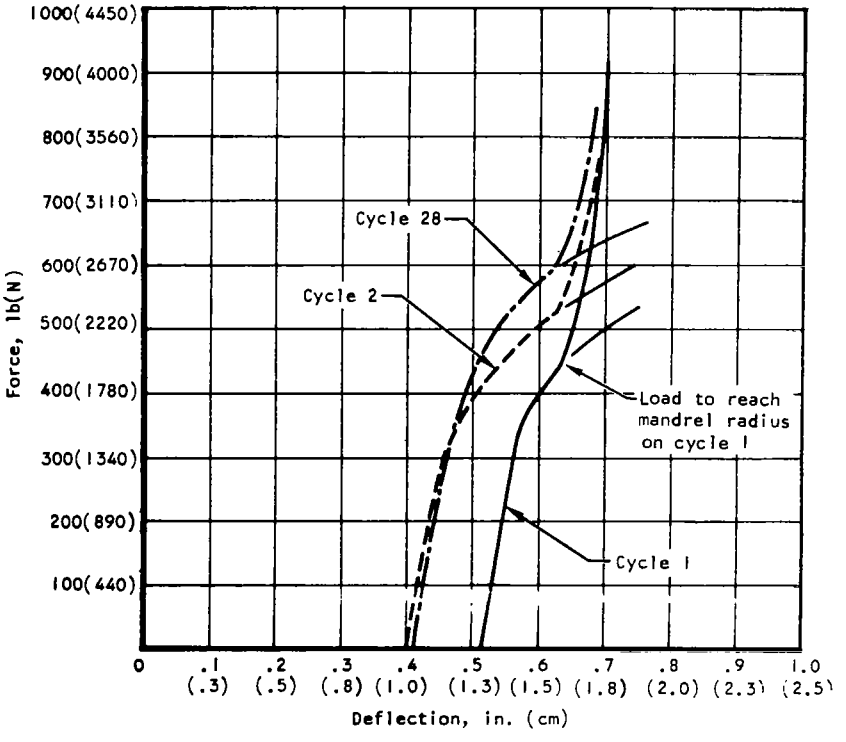

b. Typical Hastelloy X Plate-Fin Specimen Tested on a 16-in. (41 cm) Mandrel at 1340°F (1000°K)

Figure 6. Specimen Load-Deflection Cycle

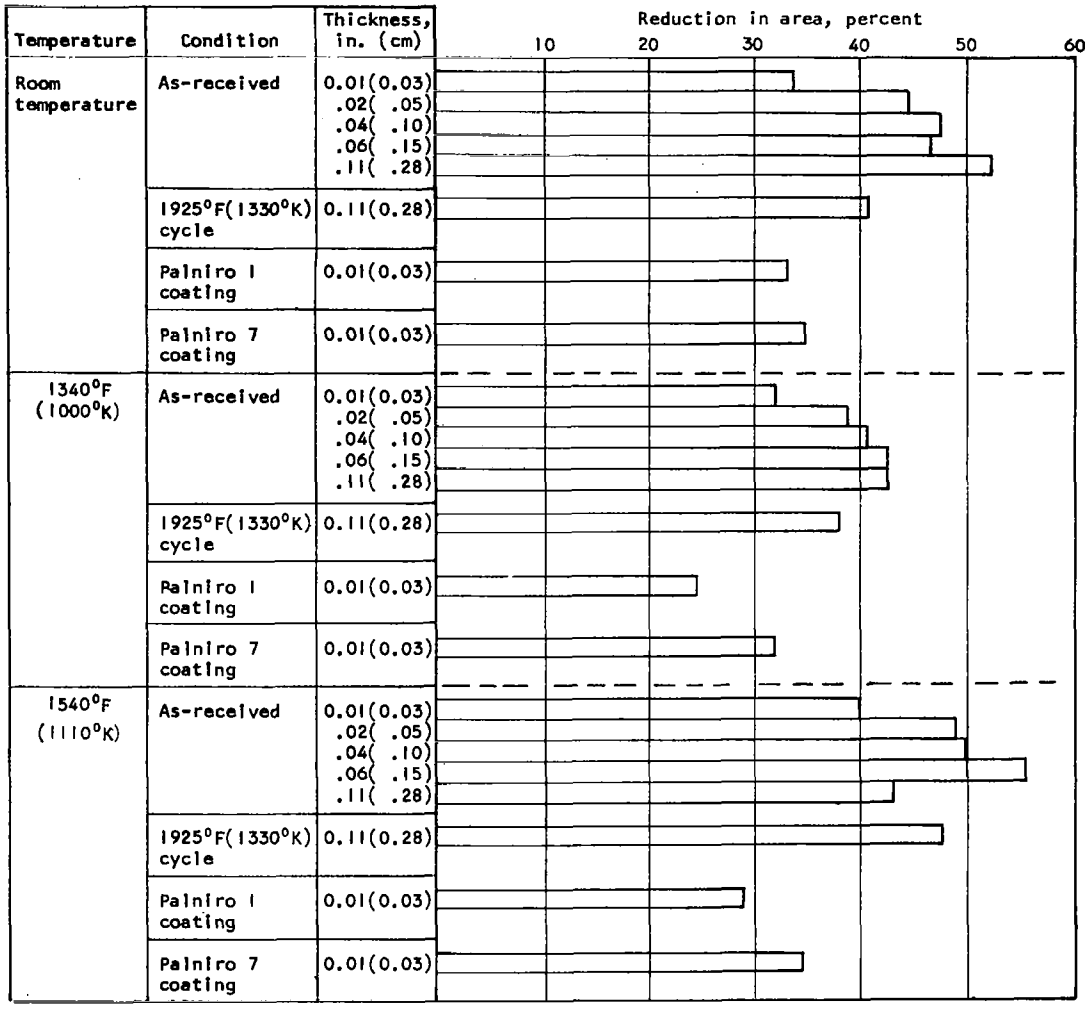

a. Ductility

Figure 7. Hastelloy X Sheet Tensile Properties

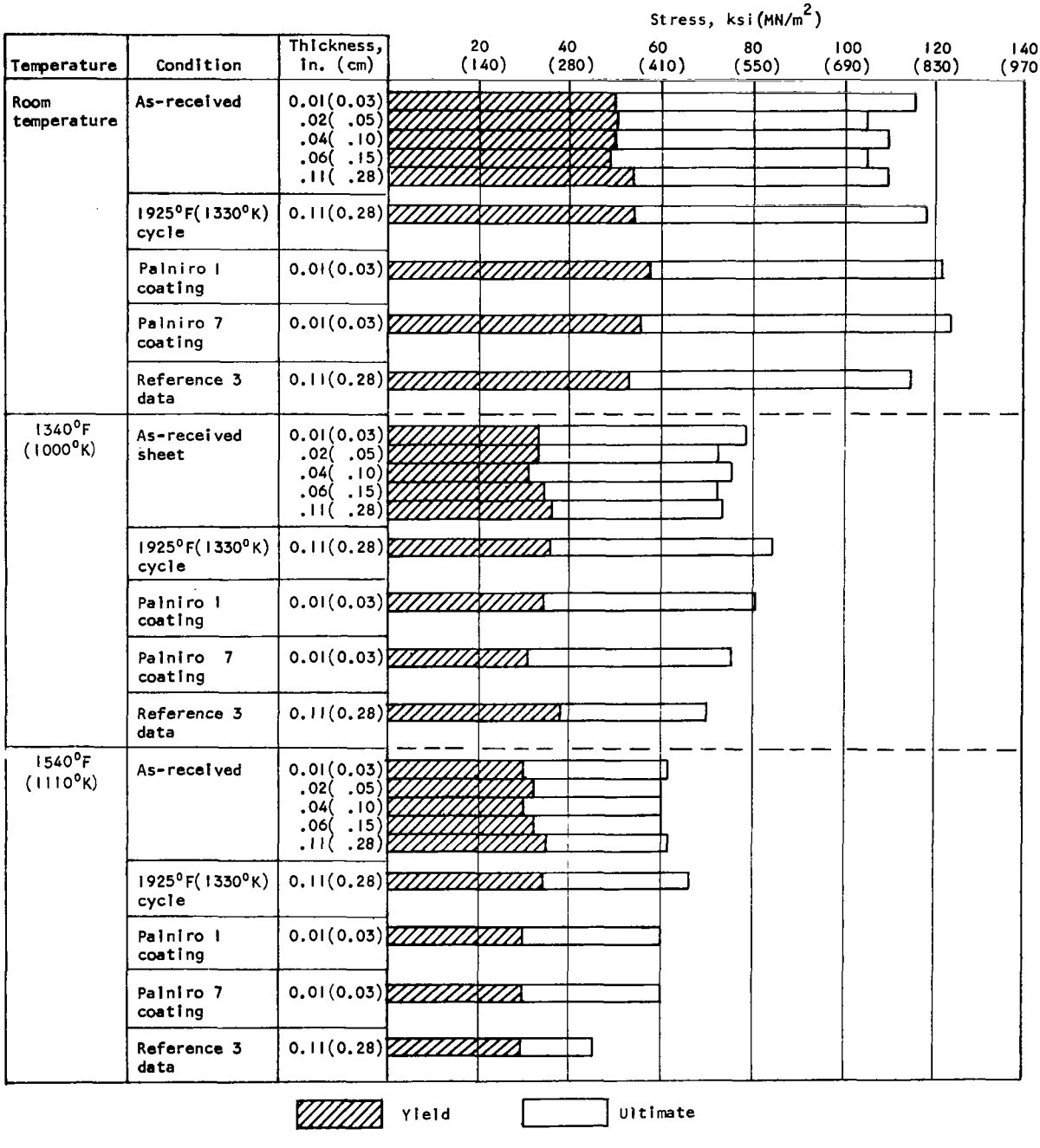

b. Tensile Strength

Figure 7. Concluded

Temperature	Condition	Thickness, in. (cm)
Room temperature	As-received	0.01(0.03) .02(.05) .04(.10) .07(.18) .11(.28)
	1925°F(1330°K) cycle	0.11(0.28)
	Palniro 1 coating	0.01(0.03)
	Palniro 7 coating	0.01(0.03)
1340°F (1000°K)	As-received	0.01(0.03) .11(.28)
	1925°F(1330°K) cycle	0.11(0.28)
	Palniro 1 coating	0.01(0.03)
	Palniro 7 coating	0.01(0.03)
1540°F (1110°K)	As-received	0.01(0.03) .11(.28)
	1925°F(1330°K) cycle	0.11(0.28)
	Palniro 1 coating	0.01(0.03)
	Palniro 7 coating	0.01(0.03)

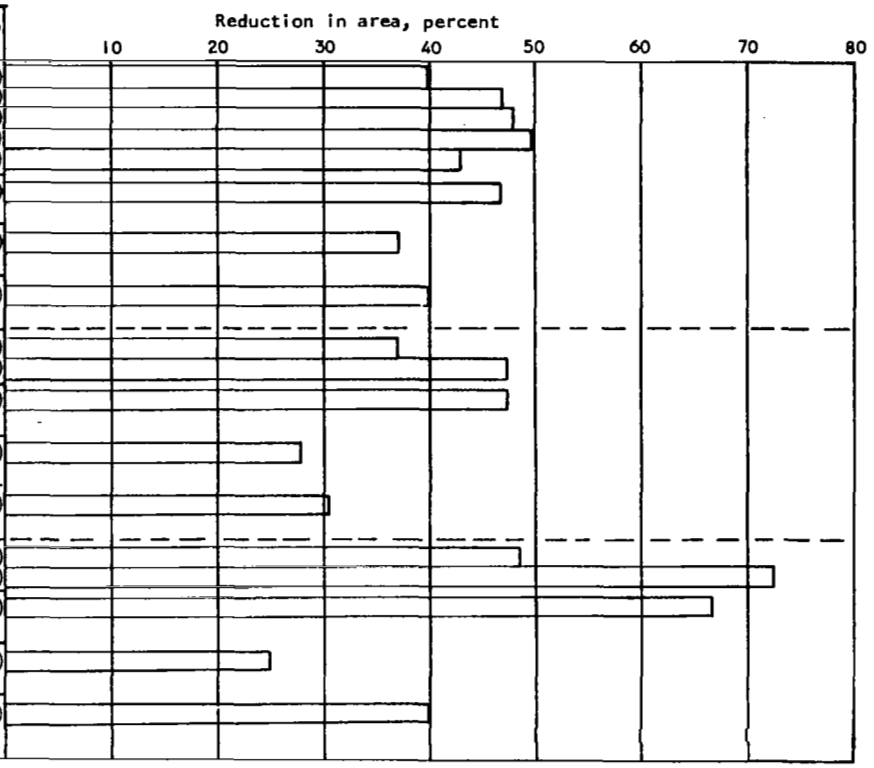

a. Ductility

Figure 8. Inconel 625 Sheet Tensile Properties

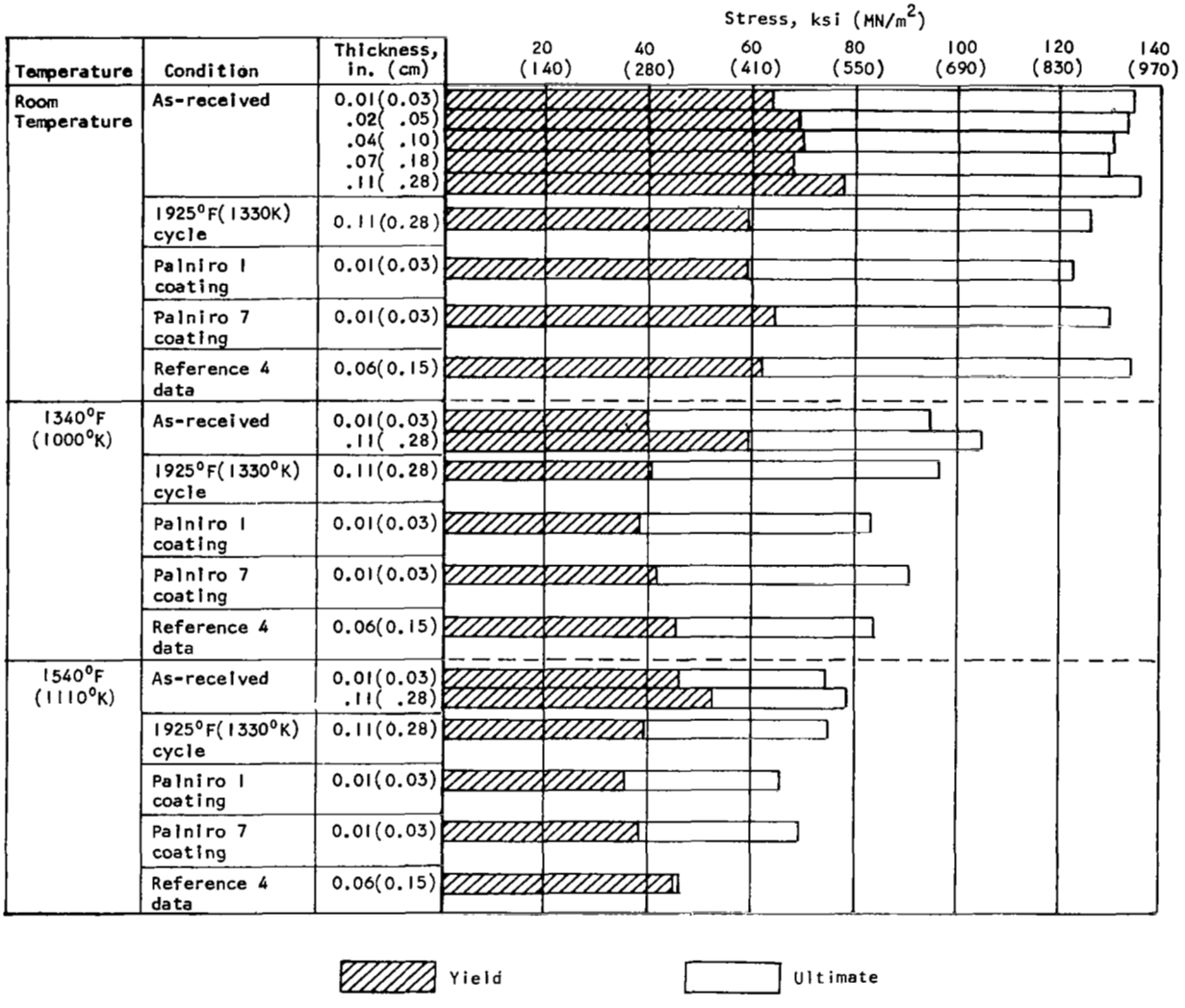

b. Tensile Strength

Figure 8. Concluded

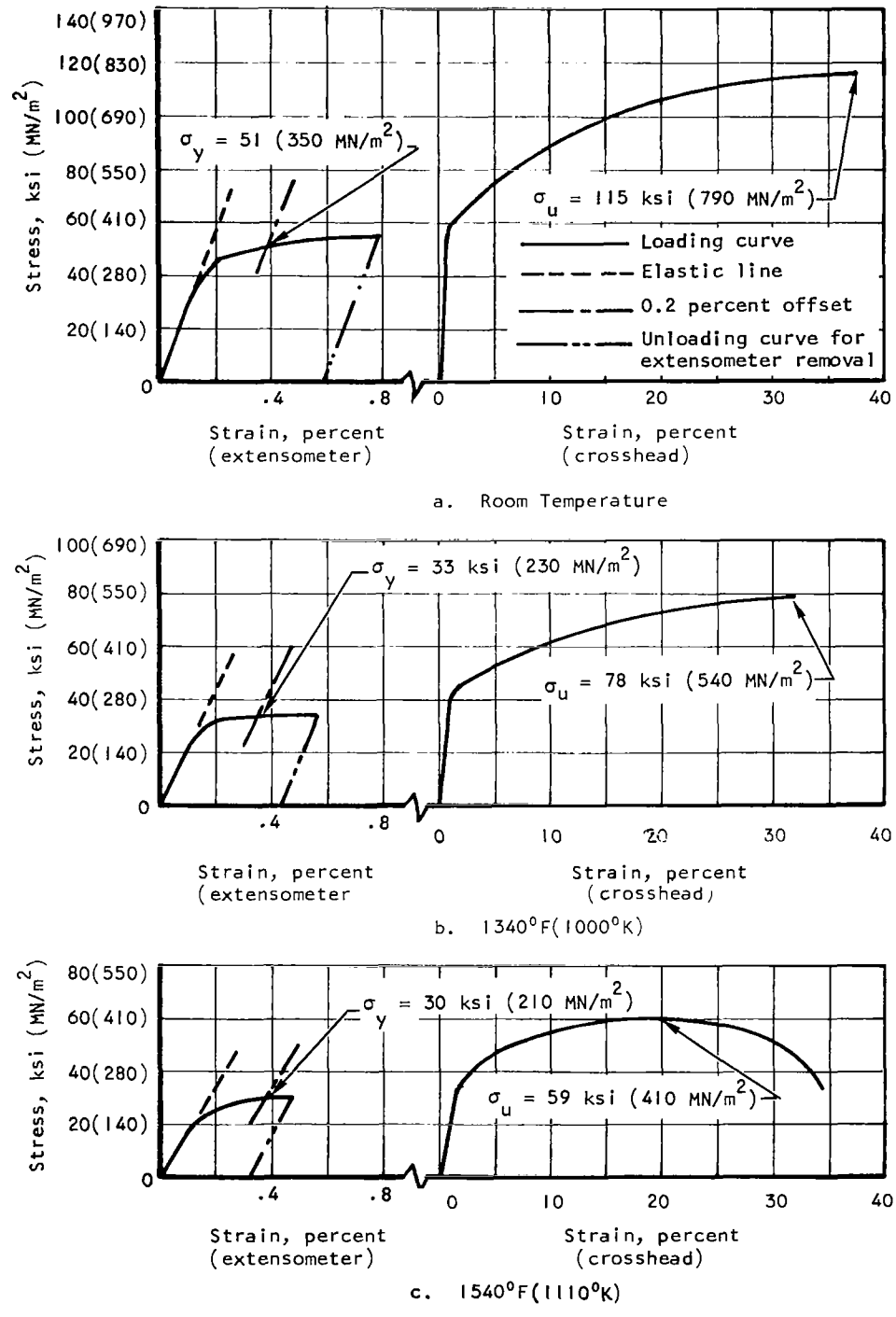

Figure 9. Typical Hastelloy X Engineering Stress-Strain Curves (As received, 0.01-in. (0.03 cm) Sheet)

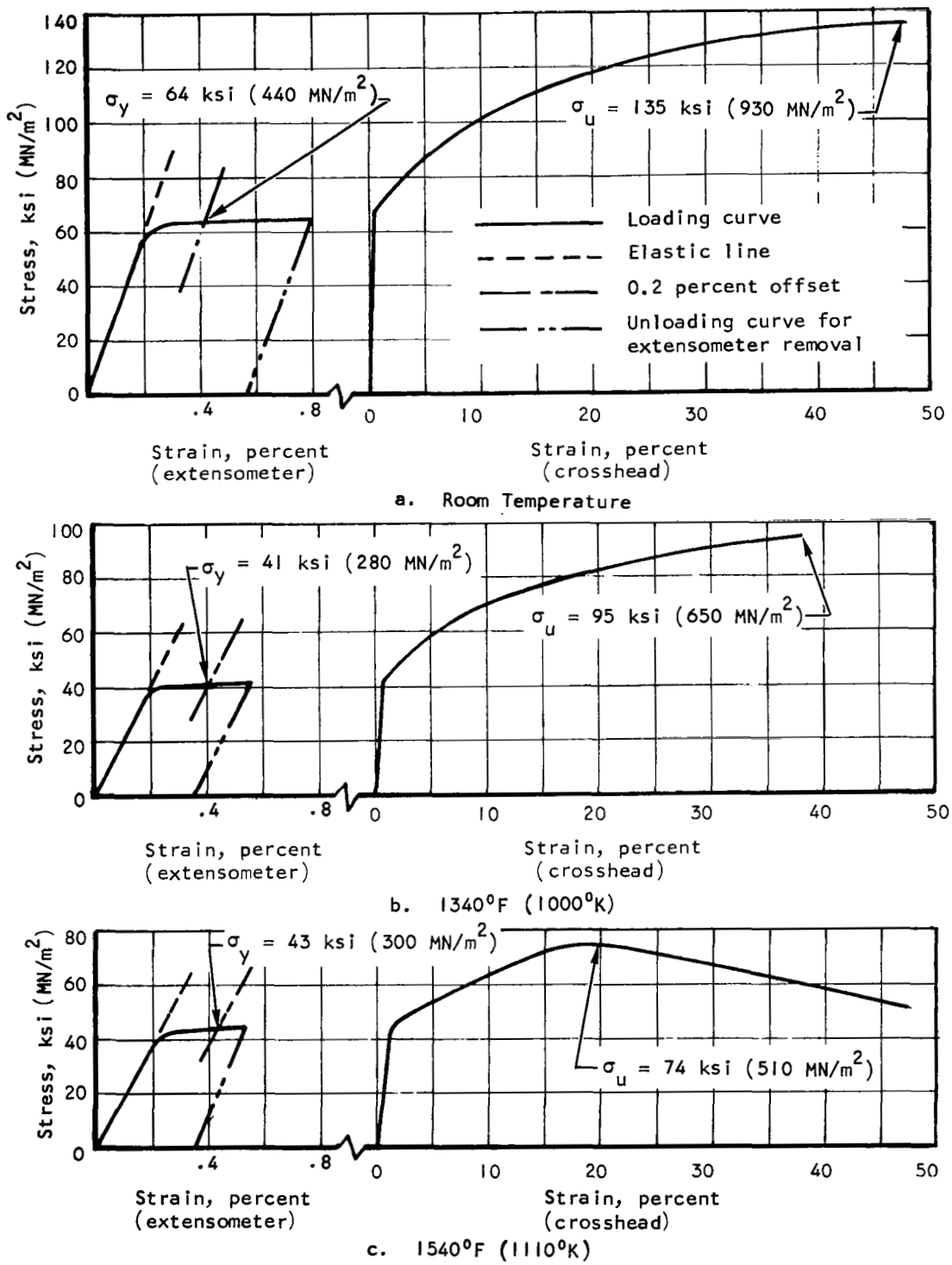

Figure 10. Typical Inconel 625 Engineering Stress-Strain Curves (As received, 0.008-in. (0.020 cm) Sheet)

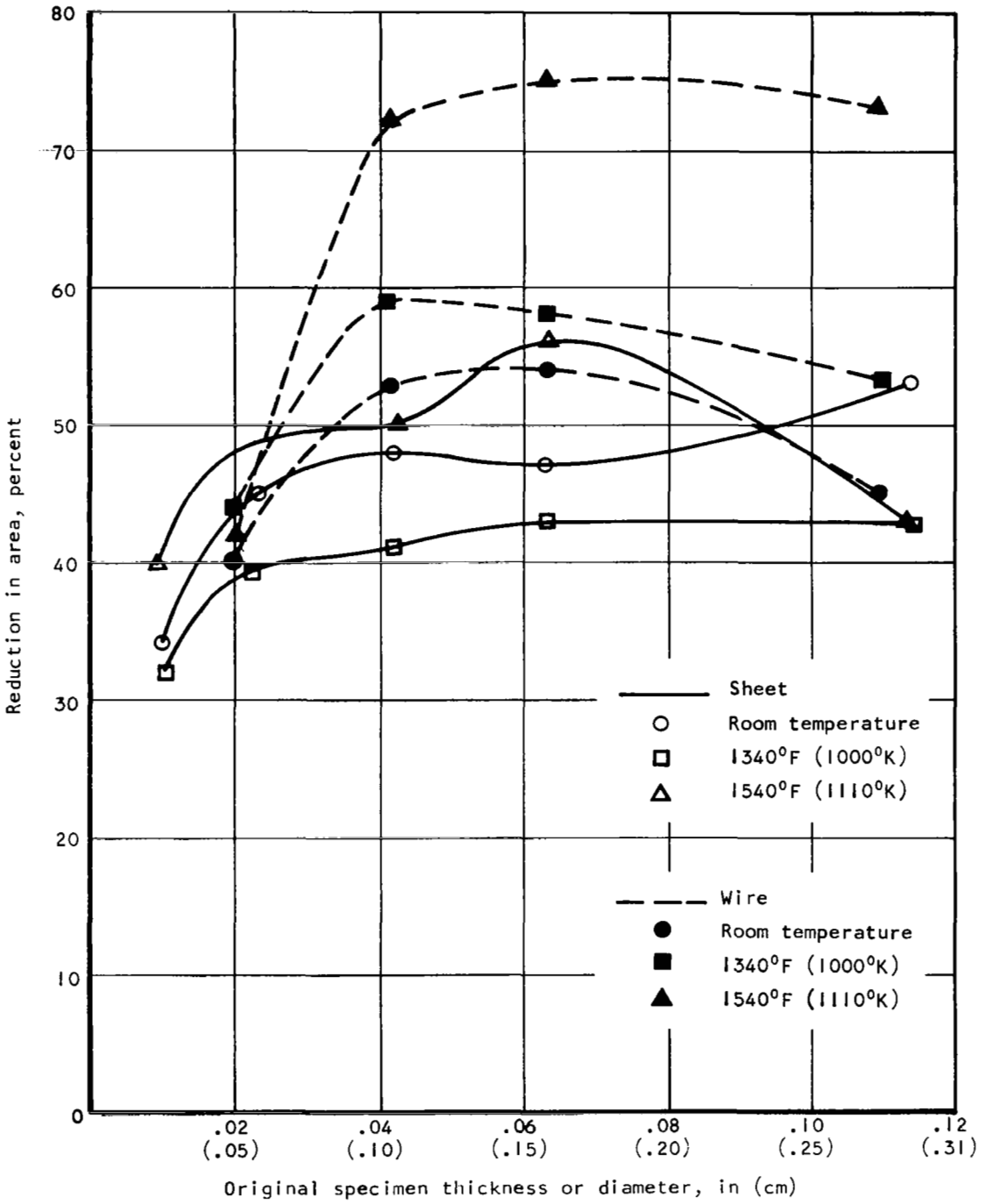

Figure 11. Hastelloy X Sheet and Wire Reduction in Area Properties vs Sheet Thickness and Wire Diameter at Three Temperatures

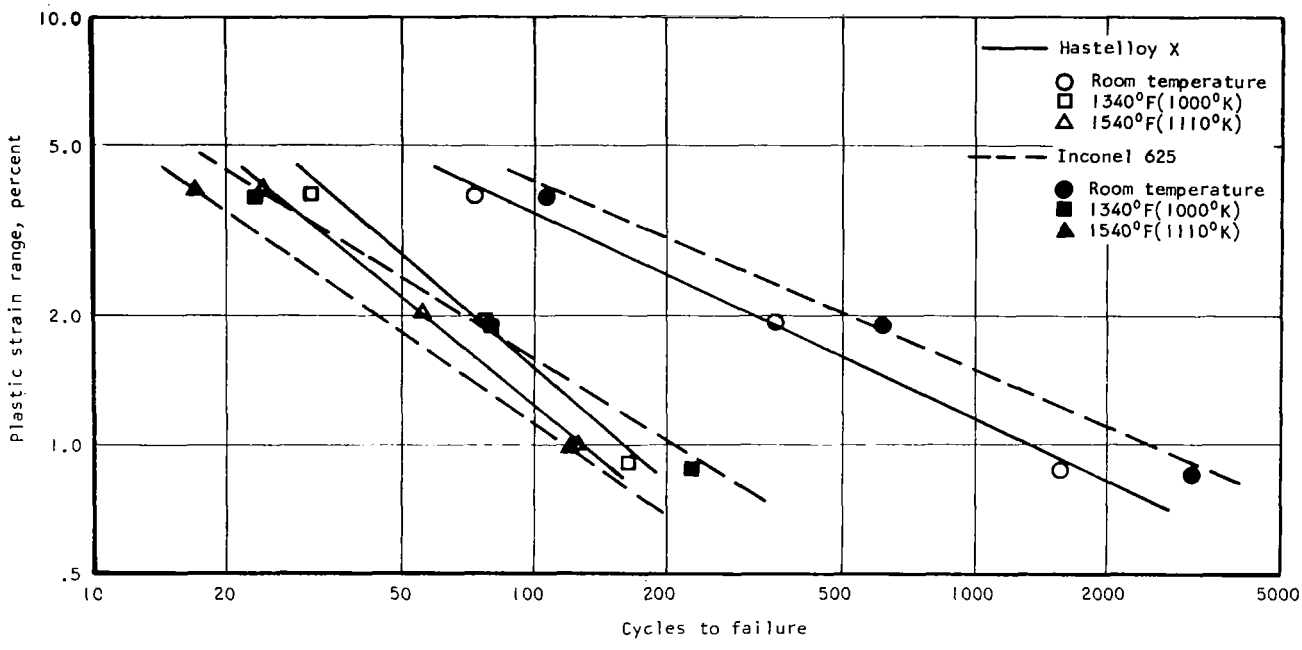

a. Fracture Depth of 0.01-in. (0.03 cm), Cavity Specimens

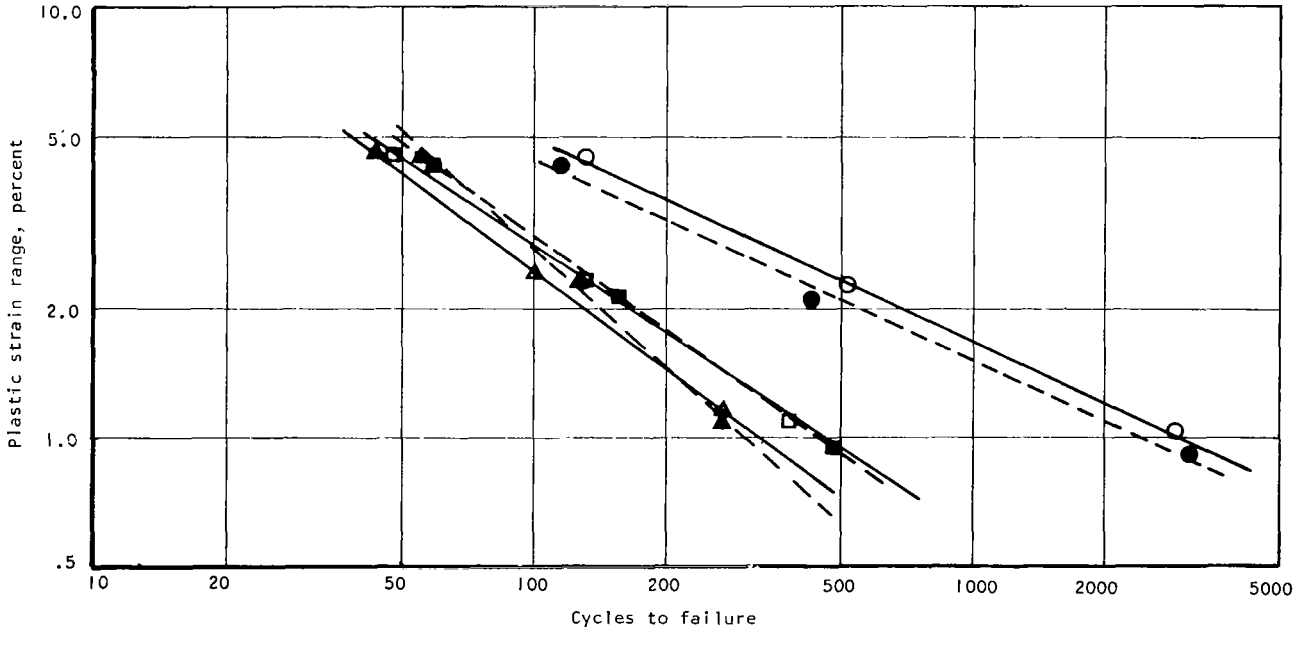

b. Fracture Depth of 0.24-in. (0.61 cm), Solid Specimens

Figure 12. Parent Metal Fatigue Summary

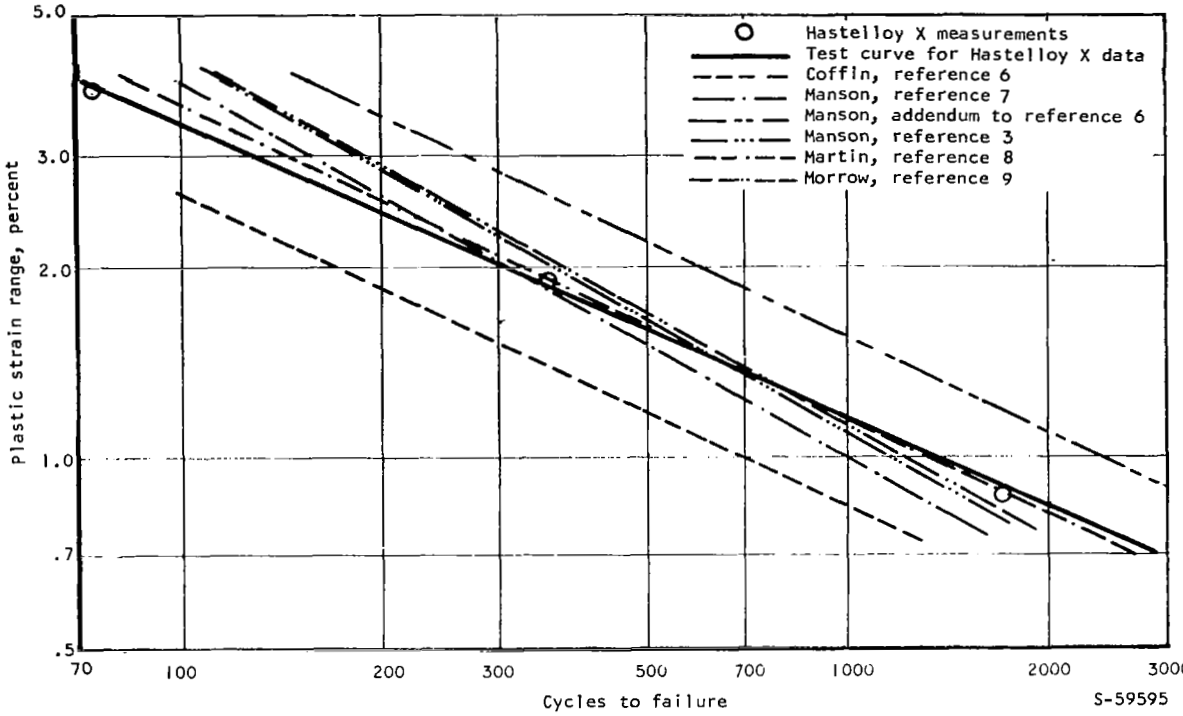

a. Hastelloy X with Measured Reduction in Area of 41 percent

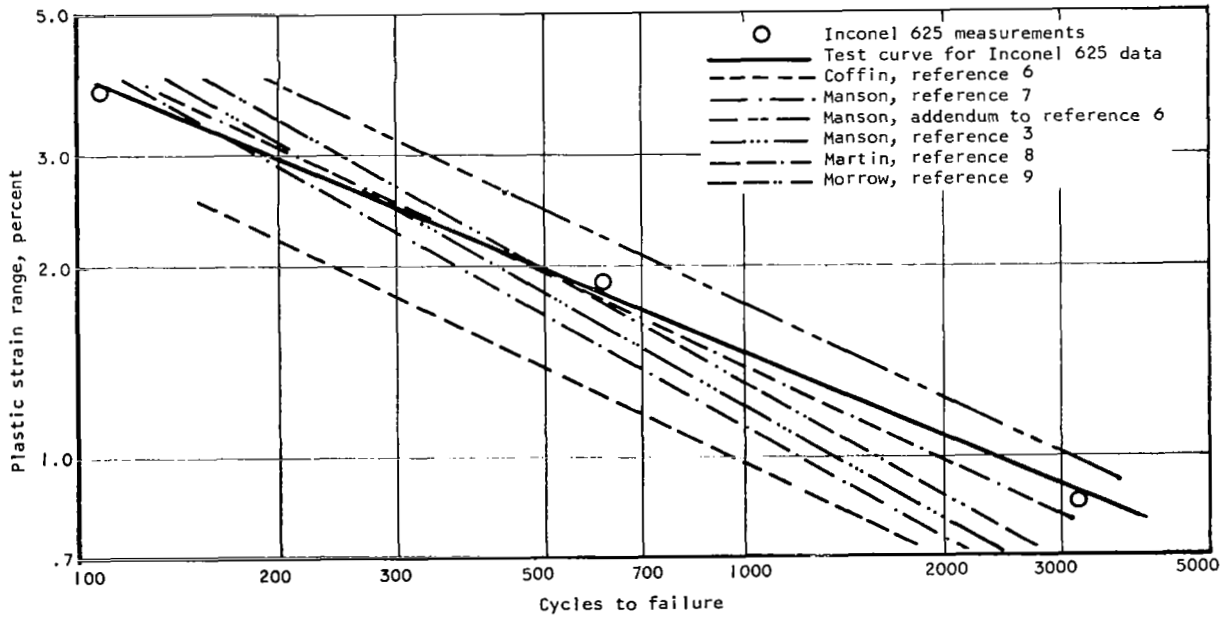

b. Inconel 625 with Measured Reduction in Area of 47 percent

Figure 13. Comparison of Cavity Specimen Fatigue Life at Room Temperature to Theoretical Predictions

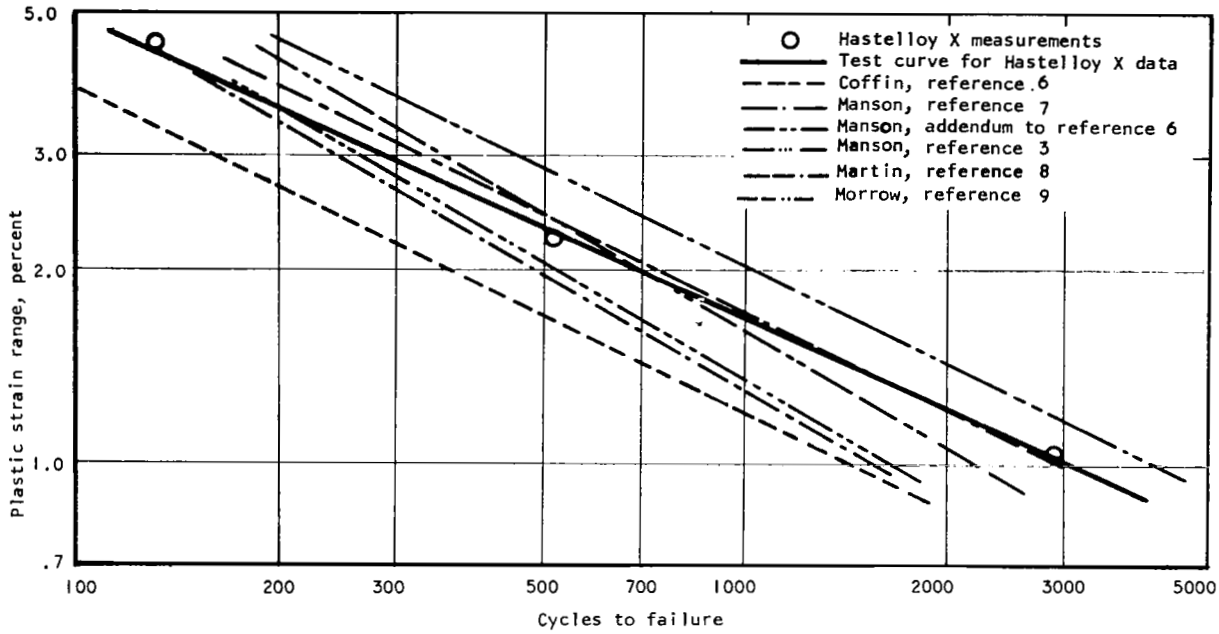

a. Hastelloy X With Measured Reduction in Area of 53 Percent

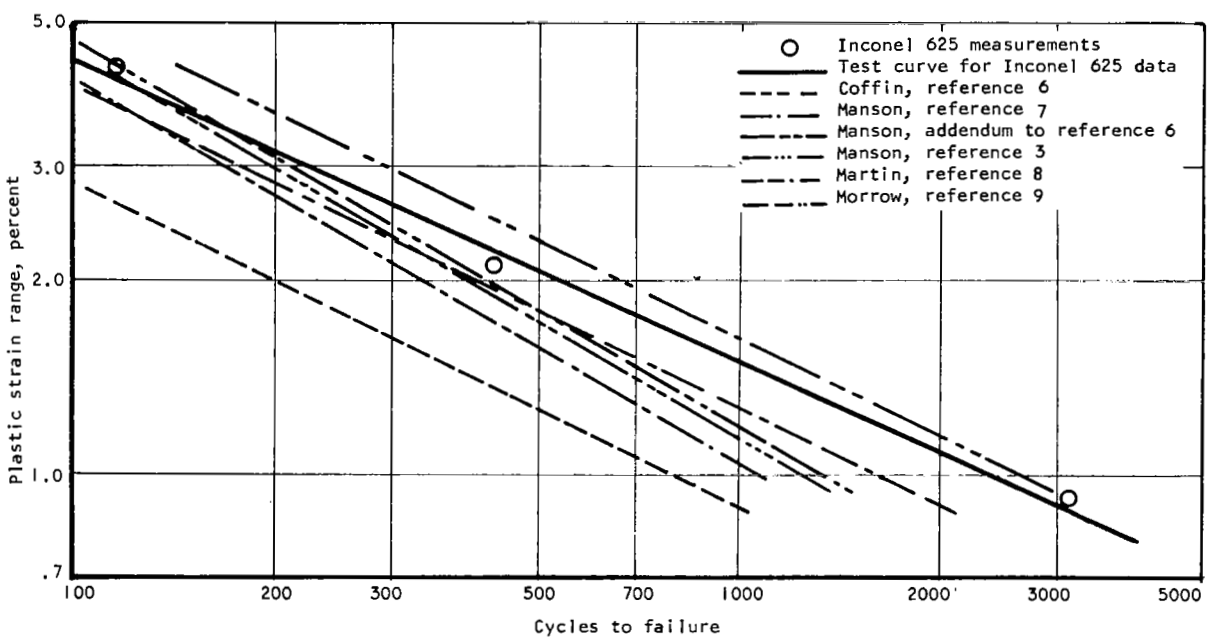

b. Inconel 625 With Measured Reduction in Area of 43 Percent

Figure 14. Comparison of Solid Specimen Fatigue Life at Room Temperature to Theoretical Predictions

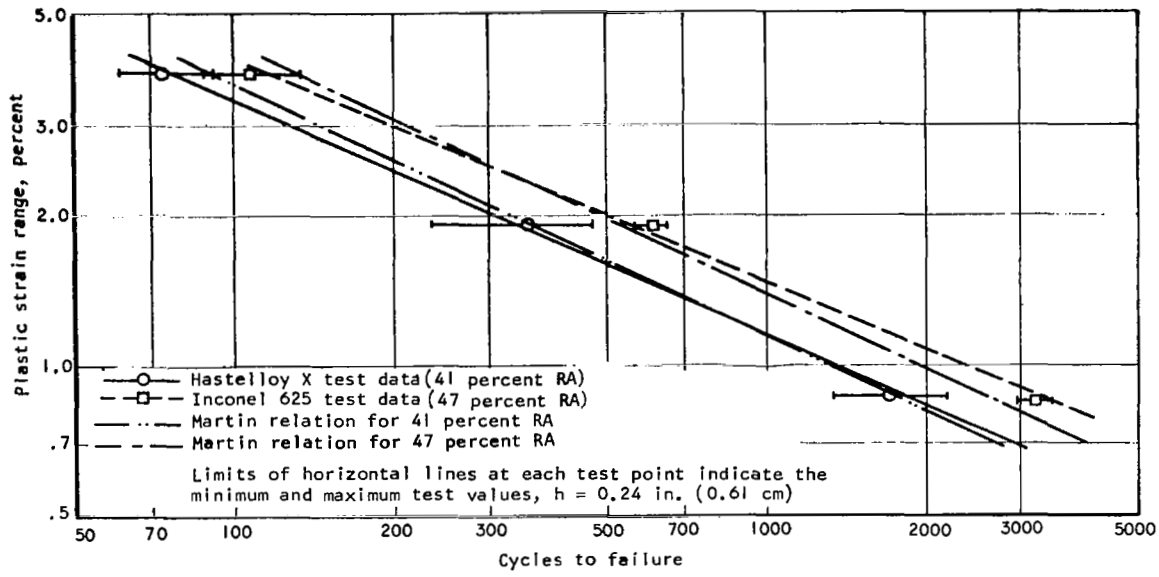

a. Cavity Specimens

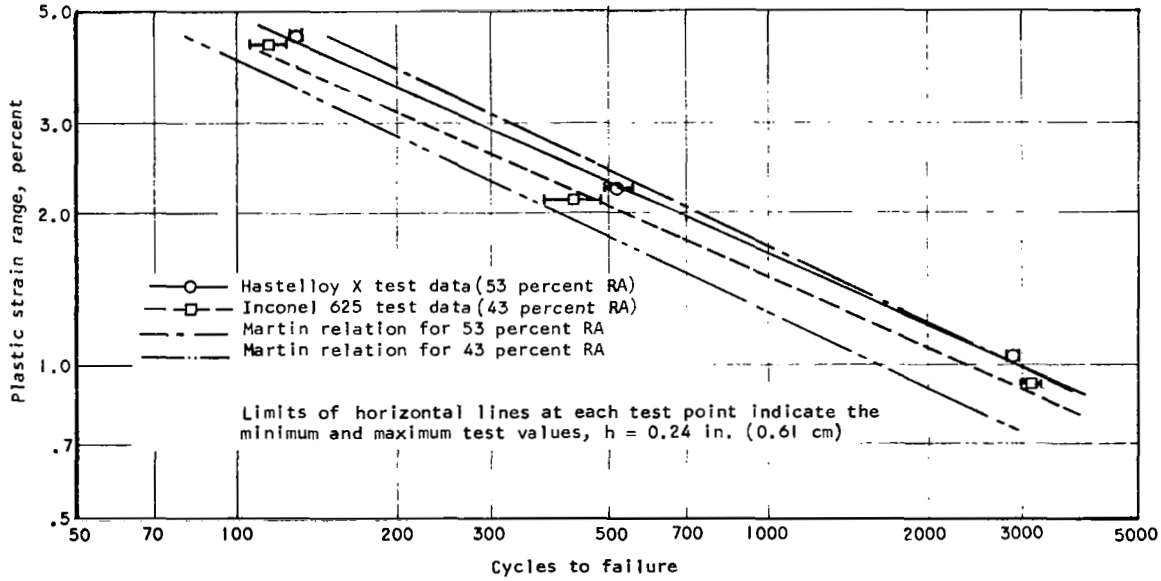

b. Solid Specimens

Figure 15. Comparison of Room Temperature Test Data to Martin Predictions

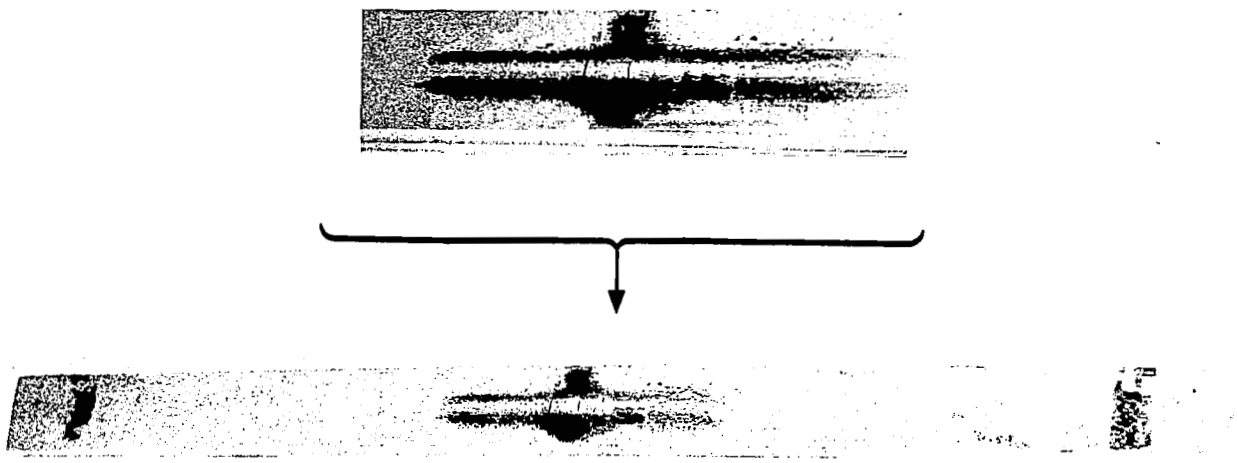

a. Cavity Specimen

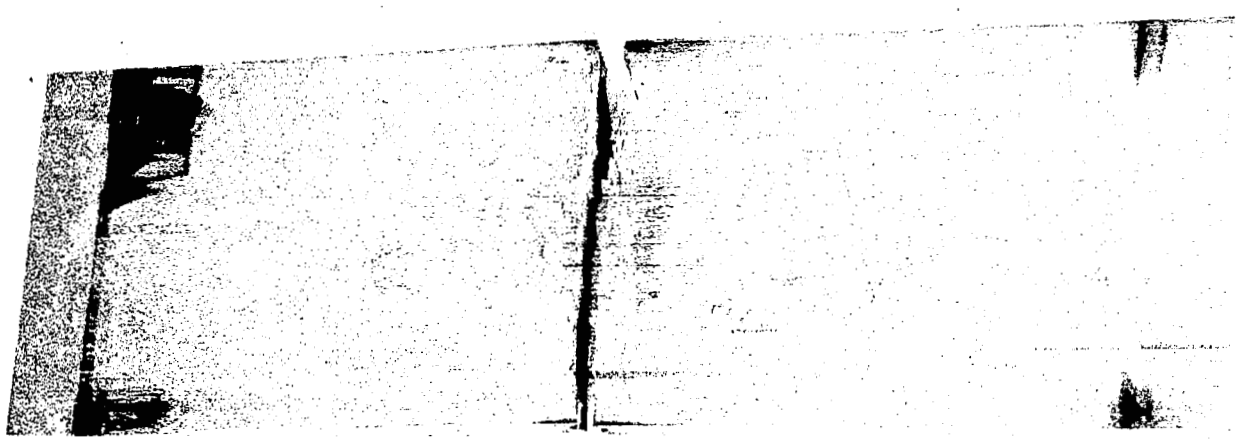

b. Solid Specimen After Full Break

Figure 16. Typical Parent Metal Specimen Failures

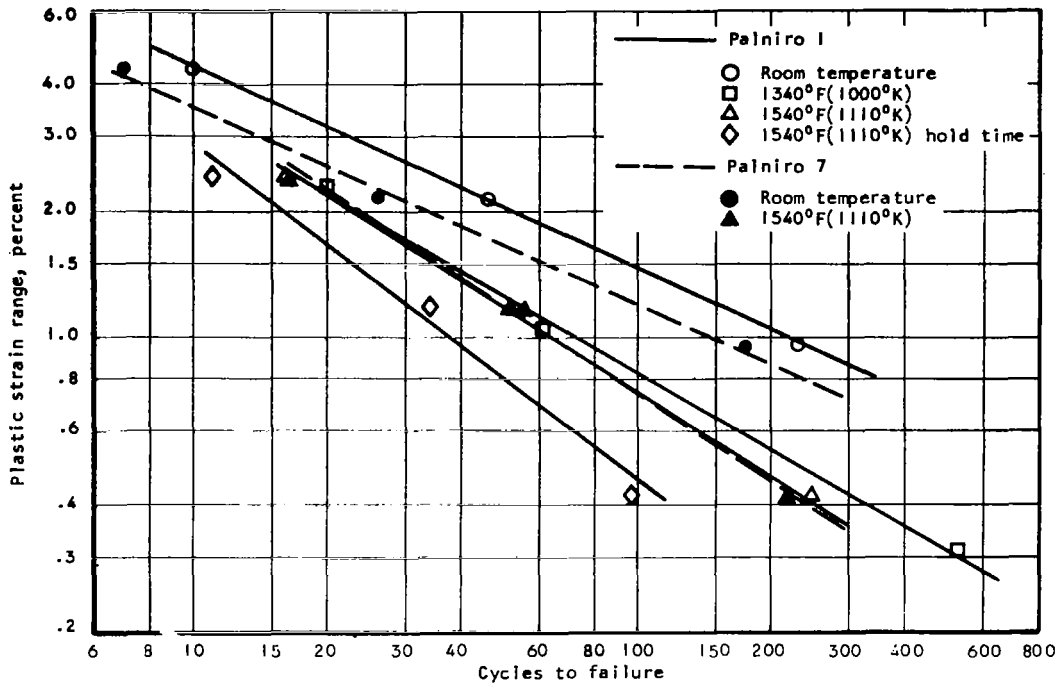

a. Hastelloy X

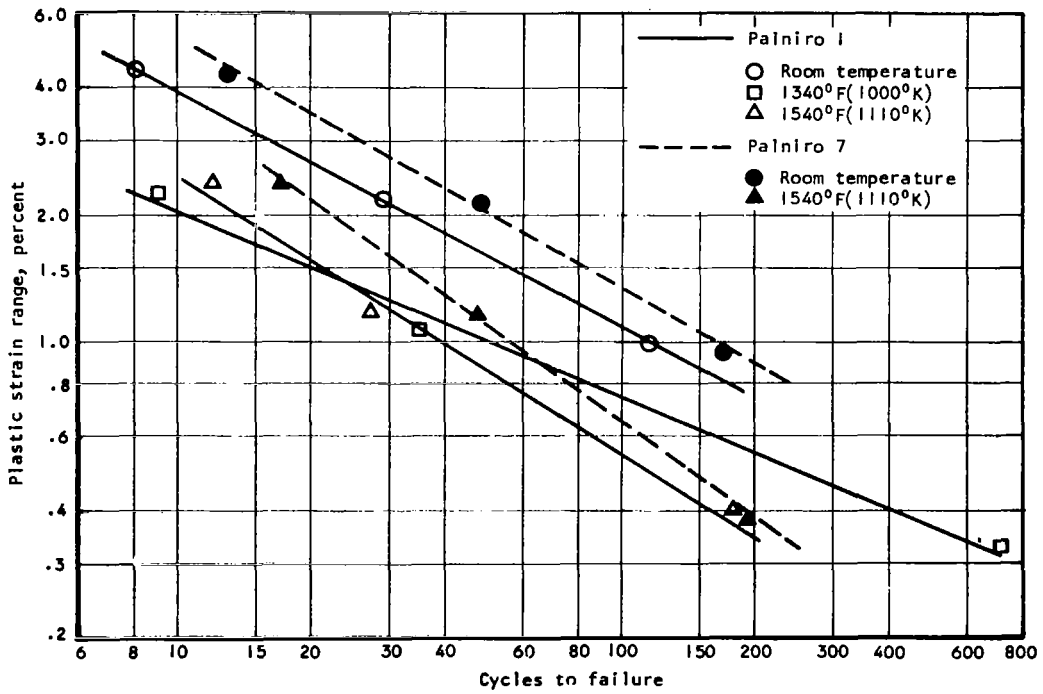

b. Inconel 625

Figure 17. Plate-Fin Fatigue Summary

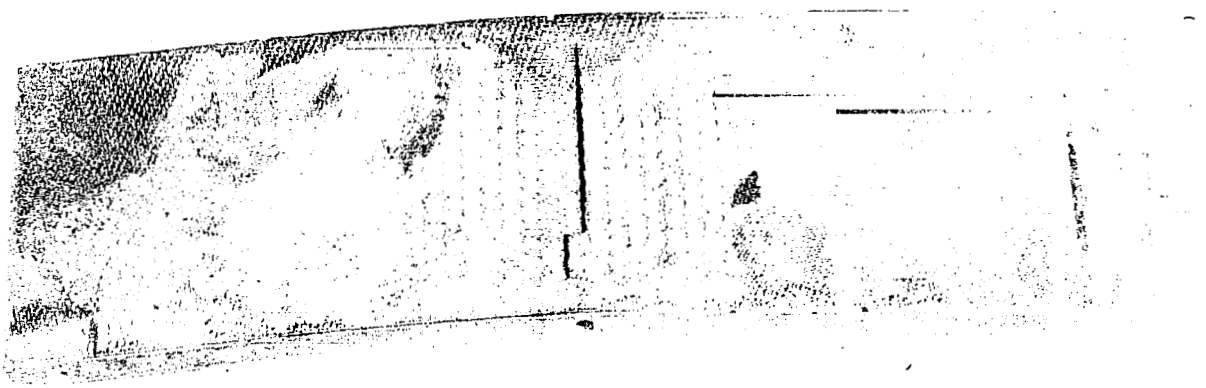

a. Typical failure

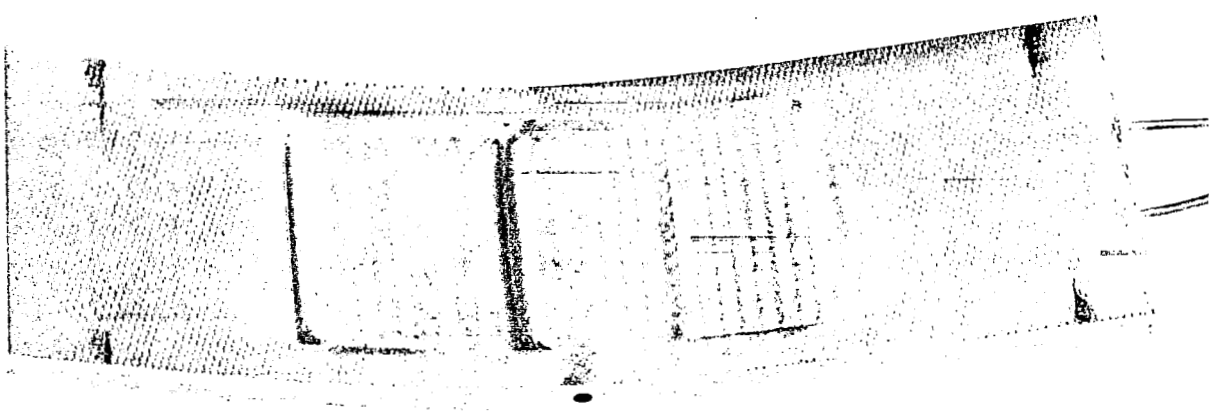

b. Failure with fin buckling

Figure 18. Typical Plate-Fin Specimen Fatigue Failures

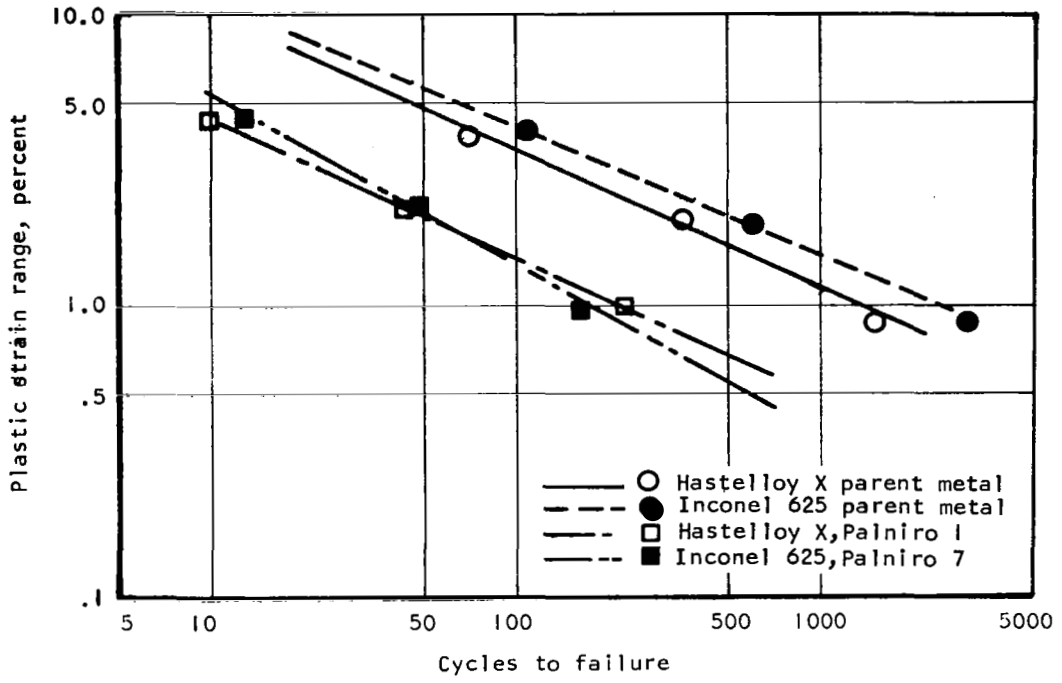

a. Room temperature

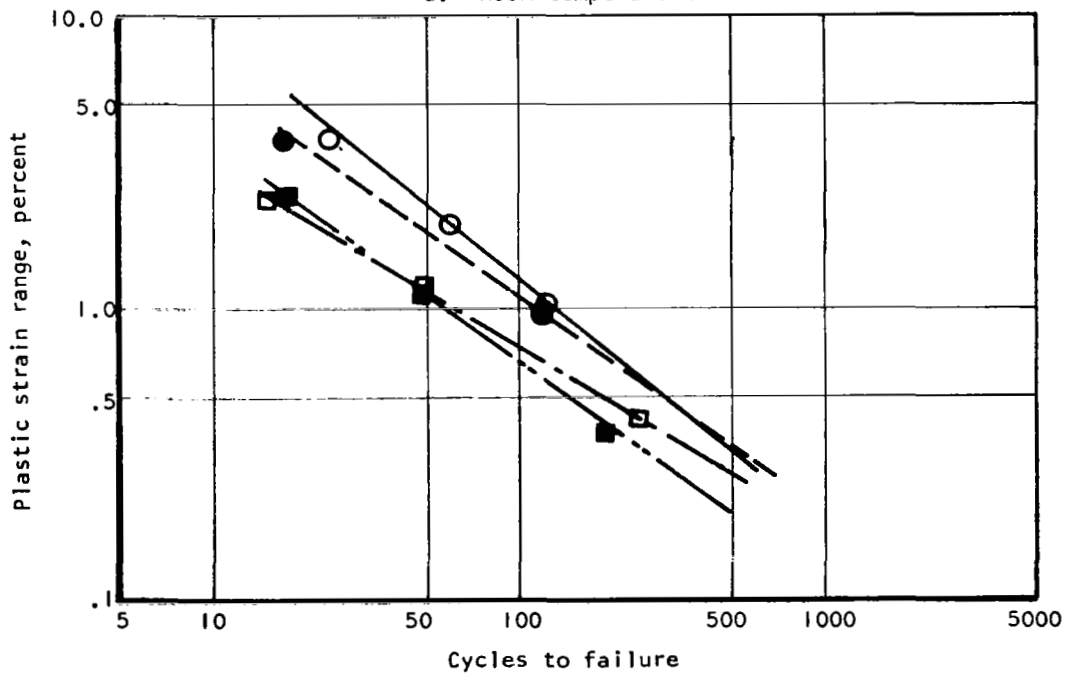

b. 1540°F (1110°K)

Figure 19. Cavity Parent Metal and Plate-Fin Fatigue Test Comparison

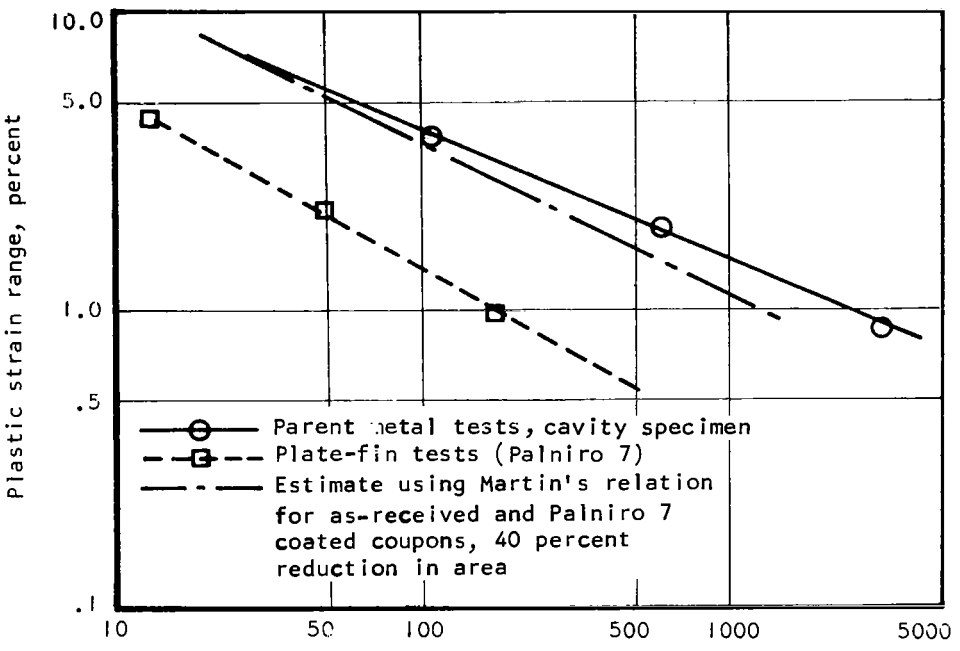

a. Inconel 625

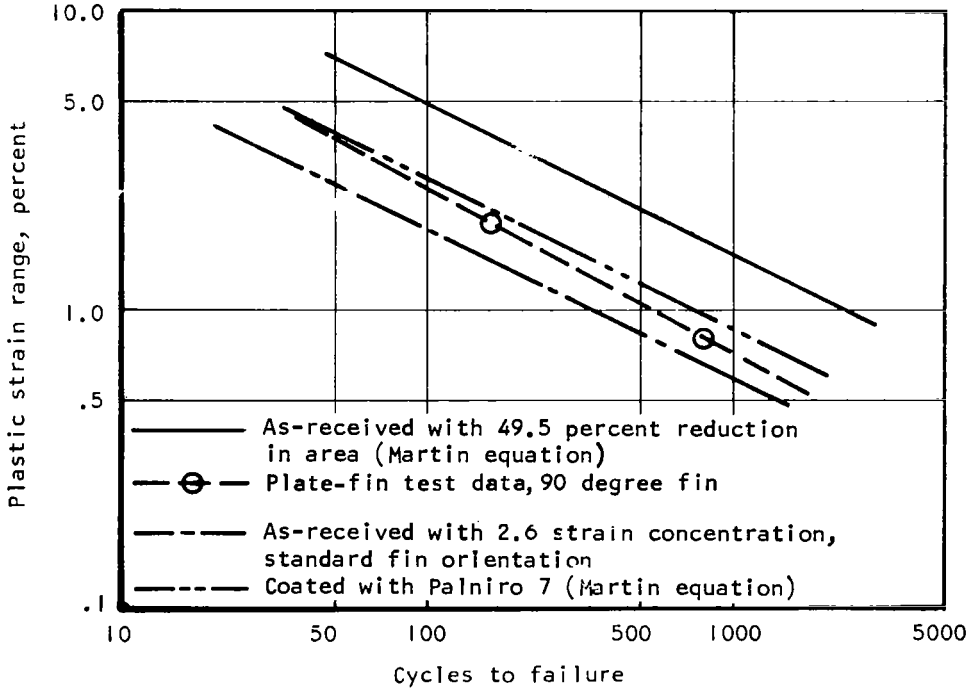

b. Inconel X-750

Figure 20. Comparative Fatigue Life of As-received, Coated and Plate-Fin Specimens

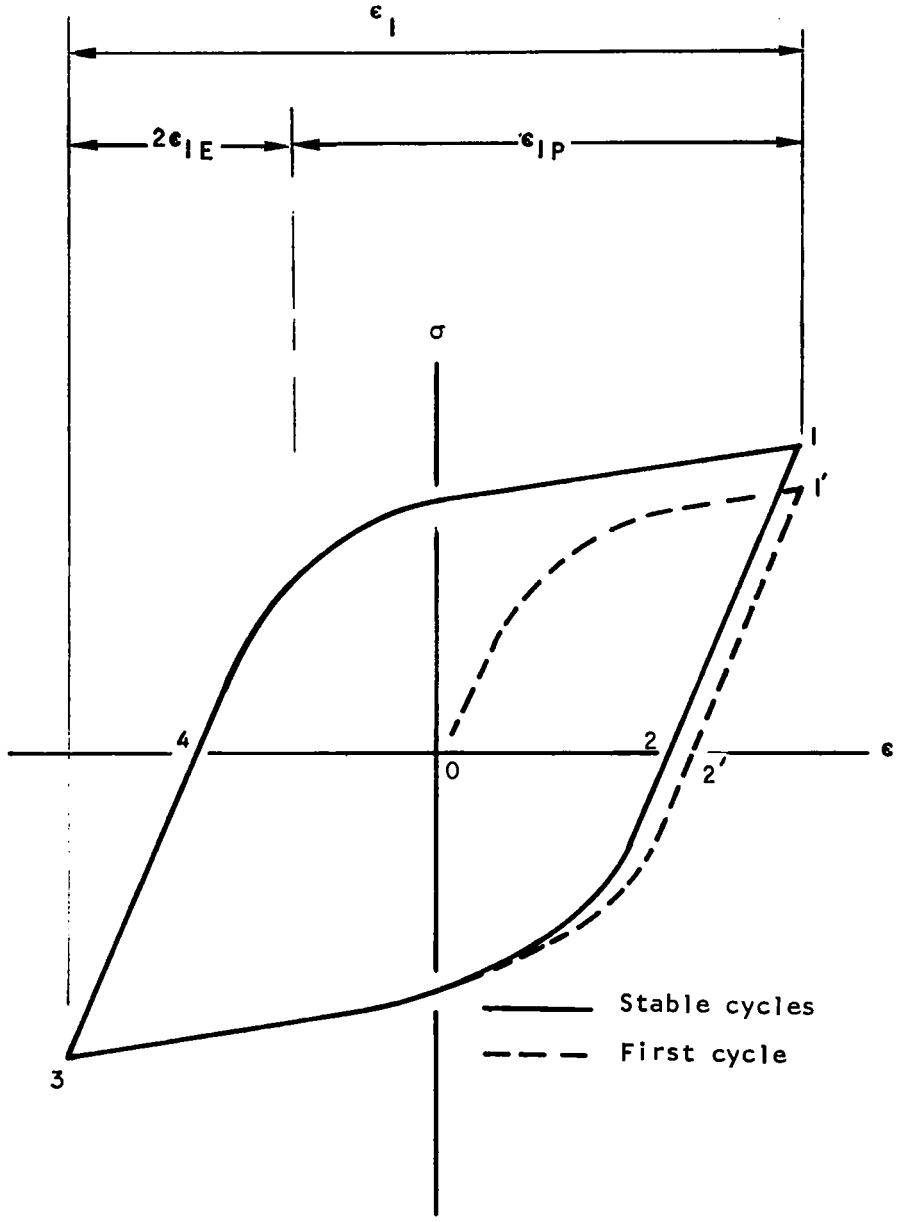

Figure 21. Assumed True Stress-Strain Cyclic Behavior, Lengthwise Component

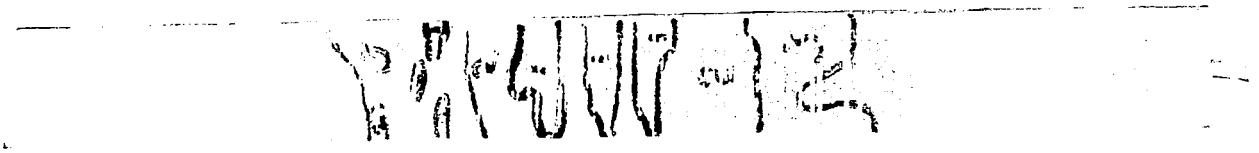

a. Stress coat result

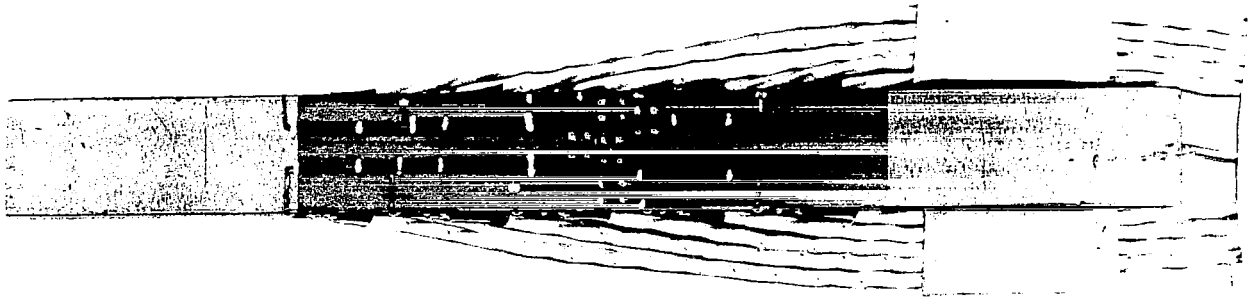

b. Strain gauge specimen

Figure 22. Stresscoat and Strain Gauge Specimens

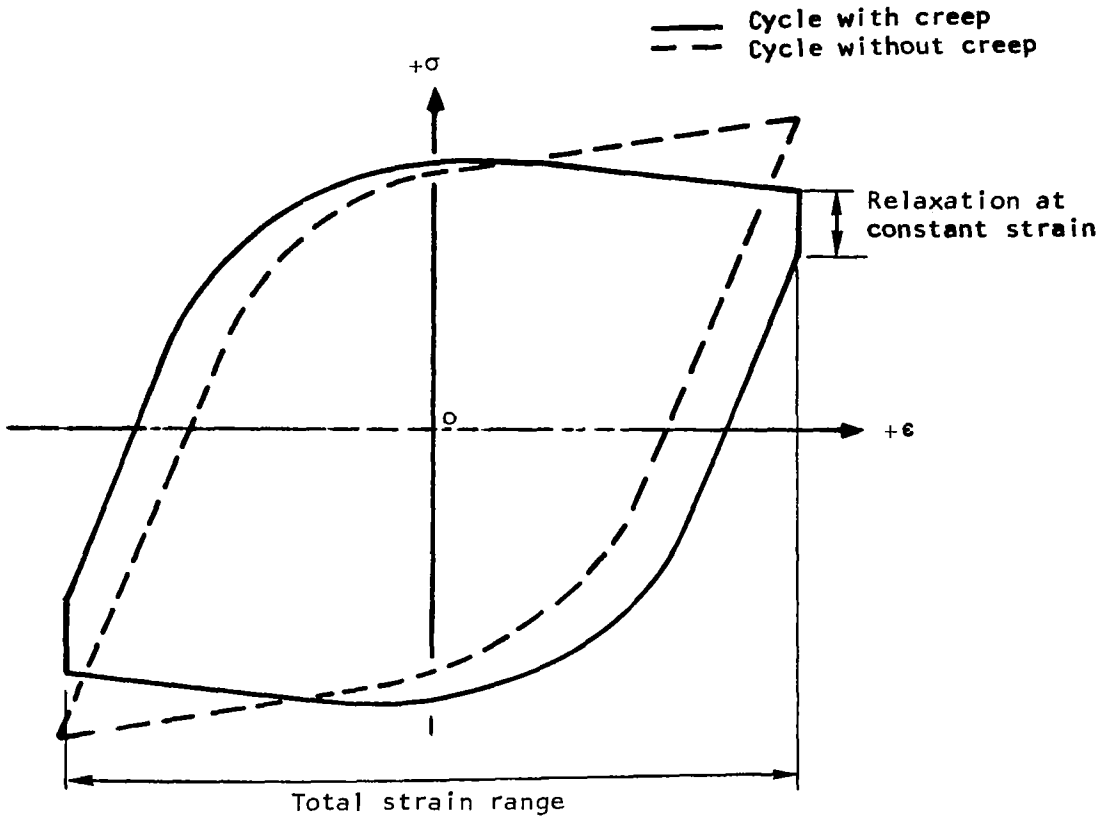

a. Complete Cycles

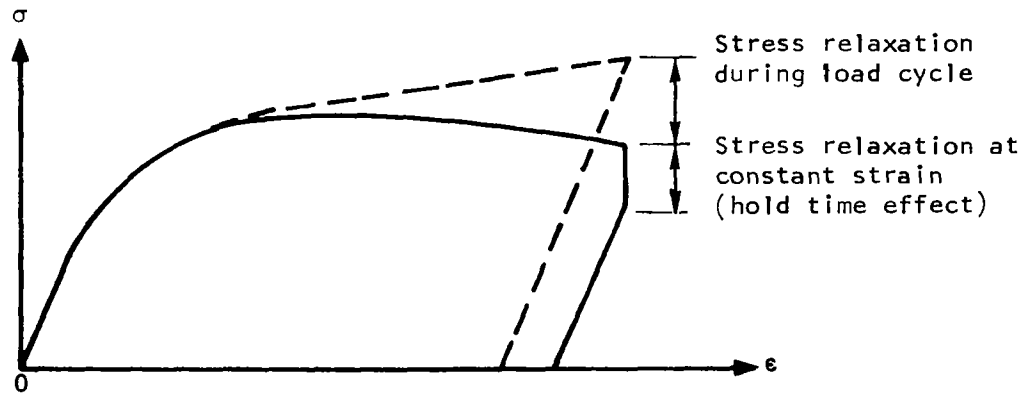

b. Cycle for Creep Damage Estimate

Figure 23. Comparison of Material Stress-Strain Behavior With and Without Creep Relaxation

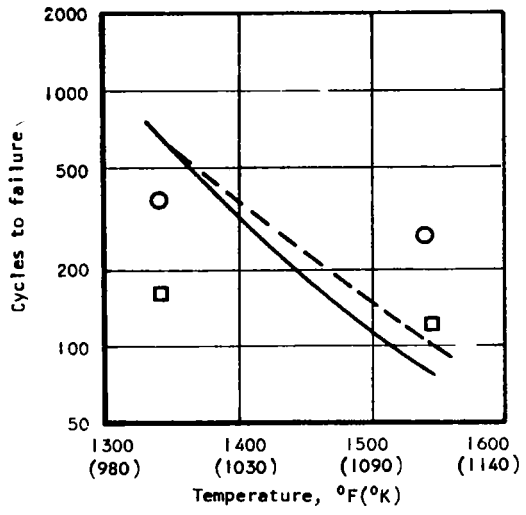

a. Life vs Temperature on the 16-in. (41 cm) Mandrel

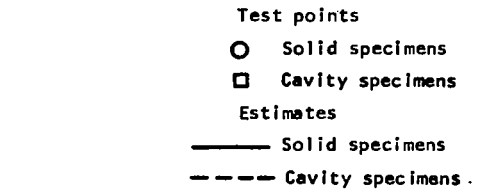

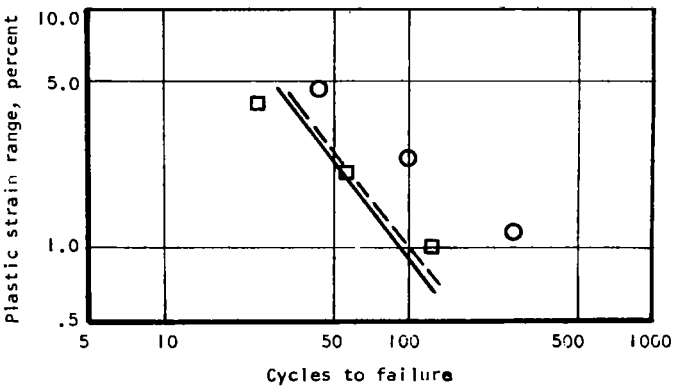

b. Life vs Plastic Strain Range at 1540°F(1110°K)

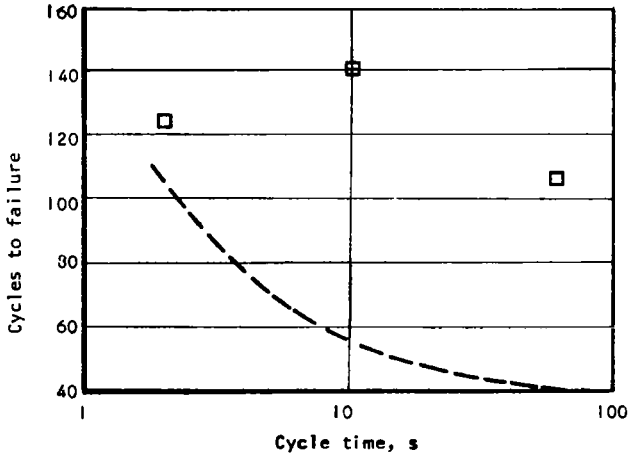

c. Life vs Cycle Time at 1540°F (1110°K), Cavity Specimen on 16-in. (41 cm) Mandrel

Figure 24. Comparison of Estimating Method to Hastelloy X Parent Metal Test Data